Cytochrome P450scc-dependent metabolism of 7-dehydrocholesterol in placenta and epidermal keratinocytes

Andrzej T. Slominski[1], **Tae-Kang Kim**[1], **Jianjun Chen**[2], **Minh N. Nguyen**[3], **Wei Li**[2], **Charles R. Yates**[2], **Trevor Sweatman**[4], **Zorica Janjetovic**[1], and **Robert C. Tuckey**[3]

[1]Department of Pathology and Medicine (AS), University of Tennessee HSC, Memphis, TN, USA

[2]Department of Pharmaceutical Sciences, University of Tennessee HSC, Memphis, TN, USA

[3]School of Biomedical, Biomolecular and Chemical Sciences, The University of Western Australia, Crawley, WA, Australia

[4]Department of Pharmacology, University of Tennessee HSC, Memphis, TN, USA

Abstract

The discovery that 7-dehydrocholesterol (7DHC) is an excellent substrate for cytochrome P450scc (CYP11A1) opens up new possibilities in biochemistry. To elucidate its biological significance we tested ex-vivo P450scc-dependent metabolism of 7DHC by tissues expressing high and low levels of P450scc activity, placenta and epidermal keratinocytes, respectively. Incubation of human placenta fragments with 7DHC led to its conversion to 7-dehydropregnenolone (7DHP), which was inhibited by DL-aminoglutethimide, and stimulated by forskolin. Final proof for P450scc involvement was provided in isolated placental mitochondria where production of 7DHP was almost completely inhibited by 22R-hydroxycholesterol. 7DHC was metabolized by placental mitochondria at a faster rate than exogenous cholesterol, under both limiting and saturating conditions of substrate transport, consistent with higher catalytic efficiency (k_{cat}/K_m) with 7DHC as substrate than with cholesterol. Ex-vivo experiments showed five 5,7-dienal intermediates with MS spectra of dihydroxy and mono-hydroxy-7DHC and retention time corresponding to $20,22(OH)_2$7DHC and 22(OH)7DHC. The chemical structure of $20,22(OH)_2$7DHC was defined by NMR. 7DHP was further metabolized by either placental fragments or placental microsomes to 7-dehydroprogesterone as defined by UV, MS and NMR, and to an additional product with a 5,7-dienal structure and MS corresponding to hydroxy-7DHP. Furthermore, epidermal keratinocytes transformed either exogenous or endogenous 7DHC to 7DHP. 7DHP inhibited keratinocytes proliferation, while the product of its pholytic transformation, pregcalciferol, lost this capability. In conclusion, tissues expressing P450scc can metabolize 7DHC to biologically active 7DHP with 22(OH)7DHC and $20,22(OH)_2$7DHC serving as intermediates, and with further metabolism to 7-dehydroprogesterone and (OH)7DHP.

Keywords

7-dehydropregnenolone; 7-dehydrocholesterol; CYP11A1; placenta; keratinocytes

Address for correspondence: Andrzej T. Slominski, MD, PhD, Department of Pathology and Laboratory Medicine, University of Tennessee Health Science Center, 930 Madison Avenue, RM525, Memphis, TN 38163, Tel: (901) 448-3741, Fax: (901) 448-6979, aslominski@uthsc.edu.

1. Introduction

7-Dehydrocholestrol (7DHC) serves as a precursor to both cholesterol, through enzymatic reduction of the B ring by the action of 7DHC Δ-reductase (Miller and Auchus, 2011, Tint et al., 1994), and to vitamin D3 through physicochemical process induced by ultraviolet light B (Holick, 2003). Until recently it was thought that cytochrome P450scc (CYP11A1) used solely cholesterol as its substrate, hydroxylating its side chain at C22 and C20, then cleaving between C20 and C22 to produce pregnenolone, a substrate for steroid hormones (Miller and Auchus, 2011, Tuckey, 2005). Recently, it was demonstrated that CYP11A1 is capable of the oxidation and cleavage of the 7DHC side chain to produce 7-dehydropregnenolone (7DHP) (Slominski et al., 2009, Slominski et al., 2004, Guryev et al., 2003), and of hydroxylating the side chain of vitamin D and ergosterol without its cleavage (Slominski et al., 2006, Slominski et al., 2005a, Slominski et al., 2005b, Guryev et al., 2003, Tuckey et al., 2008a, Nguyen et al., 2009).

A deficiency of 7DHC Δ-reductase, as seen in Smith Lemli Opitz syndrome (SLOS), leads to increased accumulation of 7DHC and production of 7DHP (Nowaczyk and Waye, 2001, Tint et al., 1994, Shackleton et al., 1999). Similarly, in vivo production of 7DHP occurs under physiological conditions during synthesis of equilin (delta-7-estrone) in horses (Tait et al., 1983), and ex-vivo in rat, rabbit, dog and pig adrenal glands (Slominski et al., 2009). 7DHP may then undergo sequential transformation to the hydroxy-derivatives of 5,7-steroidal dienes, as supported by the documented accumulation of 7DHP and its hydroxy-derivatives (including 21-hydroxy-, 17-hydroxy-, 20-hydroxy-and 17,20-dihydroxy-7DHP) in body fluids of SLOS patients (Shackleton et al., 1999, Marcos et al., 2004, Shackleton et al., 2002), and its ex-vivo transformation to the corresponding hydroxy-7DHP or 7-dehydroprogesterone in mammalian adrenal glands. 7DHP, its hydroxy-derivatives and 20(OH)7DHC are biologically active towards skin and leukemia cells (Slominski et al., 2009, Slominski et al., 2010), and as indicated by the pathological features of SLOS patients (Nowaczyk and Waye, 2001, Marcos et al., 2004, Tint et al., 1994, Smith et al., 1964).

P450scc shows relatively high expression in placenta where it initiates a local steroidogenic pathway leading to synthesis of progesterone with pregnelone as an intermediate (Tuckey, 2005). While epidermal keratinocytes accumulate significant amount of 7DHC, representing a major source of vitamin D3 for the body (Holick, 2003, Bikle, 2011), they express comparatively low levels of P450scc (Slominski et al., 2004, Slominski et al., 1996), however, sufficient to initiate a local steroidogenic pathway [reviewed in (Slominski et al., 2008, Slominski et al., 2012b)]. Furthermore, studies with the purified enzyme have shown that 7DHC is a better substrate for P450scc than cholesterol (Slominski et al., 2009). To better define the biological significance of the discovery that 7-dehydrocholesterol (7DHC) is metabolized by cytochrome P450scc (CYP11A1), being an even better substrate than cholesterol, we elucidated ex-vivo its metabolism by tissues/cells expressing high (placenta) and low (epidermal keratinocytes) CYP11A1 activities. We tested in details the ability of human placental fragments incubated ex-utero to convert 7DHC to 7DHP, and 7DHP to 7-dehydroprogesterone. We also investigated the capability of keratinocytes to produce 7DHP, including its endogenous production with preliminary assessment of the antiproliferative activity of 7DHP.

2. Materials and methods

2.1. Placentas

Term placentas (37–42 weeks) were obtained from King Edward Memorial Hospital for Women located at Crawley, WA, according to protocols approved by the hospital's human

ethics committee, or from the MedPlex in Memphis, according to protocols approved by local IRB committee at the UTHSC. The patients were 18 to 35 years old.

2.2. Incubations with human placental fragments and analysis of products

Placental fragments (parenchyma) were dissected from the membranes, washed in PBS, cut with scissors into small fragments and suspended in buffer (pH 7.4) comprising 33 mM Tris aminomethane, 110 mM NaCl, 5 mM KCl, 2.5 mM $CaCl_2$, 1 mM $MgSO_4$, 1 mM KH_2PO_4 and 2 mg/ml glucose, and incubated as described previously (Slominski et al., 2009). In total, 40 placentas were used, with 2–3 placentas being used for each experiment. Briefly, the reactions were started by adding isocitrate (5 mM), and 7-dehydrocholesterol (cholesta-5,7-dien-3β-ol; 7DHC) or 7-dehydropregnenolone (3β- hydroxypregna-5,7-dien-20-one; 7DHP) to a final concentration of 1 mM,100 μM or 10 μM as indicated. Tubes were then incubated at 37°C for various times as indicated in the Figure legends. For the majority of experiments, a 10 mM stock solution of 7DHC or 7DHP was prepared in 45% 2-hydroxypropyl-β-cyclodextrin immediately before use. In selected experiments 100 mM stock solutions were prepared in ethanol and added to the incubation mixtures at a 1:200 or 1:250 ratio. There was no difference in the metabolism of these compounds for either solvent. 7DHC was purchased from Sigma Chemical Co. (St. Louis, MO), while 7DHP was chemically synthesized and purified or photochemically transformed to pregcalciferol (pD) as described (Zmijewski et al., 2008). In control experiments, either 7DHC or 7DHP were omitted from the incubation mixture or fragments of placentas were boiled for 5 min before addition of the substrates. The reactions were stopped by placing the tubes on ice and steroids were extracted twice with methylene chloride and dried under nitrogen.

Two different HPLC and mass spectrometry systems were used to analyze incubations of placental extracts and the independent analyses confirmed the major findings of this study. First, extracts were re-dissolved in methanol and analyzed using an API-3000 LC-MS/MS (Applied Biosystems, Toronto, Canada) mass spectrometer equipped with an ESI source with Zobra Eclipse Plus C18 column (2.1 × 50 mm, 1.8 μm) (Agilent Technology, Santa Clara, CA). For initial identification of 7DHP, the elution was carried out isocratically using 85% methanol in water at a flow rate of 0.05 ml/min. The relative amount of 7DHP produced by placenta fragments was based on the intensity of the LC/MS signal (see figures 2, 4, 6–9). Both standards and placental extracts were separated and measured and under the same conditions, using a gradient of 85% to 100% methanol at 0.075 ml/min over 20 min.

The second RP-HPLC system used was a dual pump chromatograph (Waters 2695 Alliance, Milford, MA) equipped with a Waters Atlantis dC18 column (100 × 4.6 mm, 5 μm particle size). In order to detect the products of 7DHC metabolism, elution was carried out with a gradient of methanol in water (85%–100%) at a flow rate 0.5 ml/min (20 min), followed by a wash with 100% methanol (10 min). Fractions were monitored with a photodiode array detector (Waters 996, Milford, MA) and collected manually for further MS analyses. The collected samples were analyzed using an API 4000 LC-MS/MS (Applied Biosystems, Toronto, Canada) mass spectrometer equipped with an ESI source in positive mode with a declustering potential of 80 V, an entrance potential of 10 V and an ion spray voltage of 4.5 kV.

Mass spectra of intermediates generated by purified P450scc were also acquired with a Bruker Esquire-LC/MS system (Bruker Daltonics, Billerica, MA) utilizing an electrospray ionization (ESI) source. Data were collected and processed by ACD mass processor.

2.3. Measurement of 7-dehydrocholesterol and [4-^{14}C]cholesterol metabolism by placental mitochondria

A mitochondrial fraction from the placentas was prepared by differential centrifugation as described previously (Tuckey et al., 1997). Mitochondria isolated by this procedure showed minimal cytoplasmic contamination, containing only 1.9% of the total lactate dehydrogenase activity assayed by the oxidation of NADPH (0.15 mM) in the presence of 1.0 mM pyruvate. Mitochondria (0.88 mg/ml) were incubated in buffer comprising 50 mM HEPES pH 7.4, 0.25 M sucrose, 20 mM KCl, 5 mM MgSO4, 0.2 mM EDTA and 0.5 mg/ml bovine serum albumin (fatty acid free) in a final volume of 0.5 ml. Cyanoketone (8 μM) (Sterling-Winthrop Research Institute, Rensselaer, NY), a 3β-hydroxysteroid dehydrogenase inhibitor (Arthur and Boyd, 1974), was added to prevent metabolism of the pregnenolone or 7-dehydropregnenolone product, as before (Slominski et al., 2009) Mitochondria were preincubated at 37°C for 8 min then 7-dehydrocholesterol or [4-^{14}C]cholesterol (0.05 μCi) was added to the mitochondria to a final concentration of 200 μM from a 10 mM stock solution in ethanol. Reactions were then started immediately by the addition of isocitrate and NADP$^+$, to final concentrations of 5 mM and 50 μM, respectively. N-62 StAR protein (5 μM) was present for some incubations (see Results) and was added at the same time as substrate. The N-62 StAR protein, which was expressed in *Escherichia coli* (*E. coli*) (Bose et al., 2000), was provided by Walter Miller (University of California, San Francisco). Reactions were carried out for various times at 37°C (see Results) and were terminated by the addition of 2.5 ml ice-cold methylene chloride and 0.5 ml water. After centrifugation to separate phases, the lower methylene chloride phase was retained and the aqueous phase re-extracted twice more with 2.5 ml methylene chloride. The solvent was removed under nitrogen and the residue dissolved in 64% methanol for HPLC.

The extracts of mitochondria incubated with 7DHC were analyzed by reversephase HPLC using a Perkin Elmer HPLC equipped with a C18 column (Grace Smart, 15 cm × 4.6 mm). Samples were applied in 64% methanol and chromatographed using a linear gradient of 64–100% methanol in water for 15 min followed by 100% methanol for 35 min, at a flow rate of 0.5 ml/min. Products were detected with a UV monitor at 280 nm. The extracts of mitochondria incubated with [4-^{14}C]cholesterol were subjected to TLC to separate the radiolabelled cholesterol substrate from pregnenolone product, which were then quantitated by scintillation counting (Slominski et al., 2004).

2.4. 7DHC metabolism by purified human P450scc

Human P450scc, adrenodoxin reductase and adrenodoxin were expressed in *E. coli* and purified as described previously (Tuckey et al., 2008b). Human cytochrome P450scc (1.0 μM) was incubated with 200 μM 7DHC in buffer comprising 20 mM HEPES (pH 7.4), 100 mM NaCl, 0.1 mM dithiothreitol and 0.1 mM EDTA, 0.9% 2-hydroxypropyl-β-cyclodextrin (used to solubilize the 7DHC), 0.4 μM adrenodoxin reductase, 15 μM adrenodoxin and 50 μM NADPH, for 5 min at 37°C. The reaction was stopped by the addition of cold methylene chloride and steroids were extracted with methylene chloride as before (Tuckey et al., 2008b). Products were analyzed on a Grace Alltima C18 column (25 cm × 4.6 mm) with a gradient of 64–100% methanol in water for 15 min, then 100% methanol for 25 min, at 1.0 ml/min. For collection of products for further analysis, the 64–100% methanol gradient was applied for 40 min followed by 100% methanol for 45 min, at 0.5 ml/min.

2.5. Metabolism of hydroxy-7DHC intermediates by human P450scc

Hydroxy-7DHC intermediates (collected as above) were incorporated into vesicles prepared by sonication of dioleoyl phosphatidylcholine and bovine heart cardiolipin in the ratio 85:15 (mol/mol), as described previously (Tuckey et al., 2008b). Purified human P450scc (0.5 μM) was added to the vesicles and incubations carried out at 37°C for 20 min, as described in

detail previously (Tuckey et al., 2008b). HPLC separation of products was carried out on a Grace Alltima C18 column (25 cm × 4.6 mm) with a gradient of 64–100% methanol in water for 15 min, then100% methanol for 25 min, at 0.5ml/min.

2.6. Metabolism of 7DHP by placental microsomes

A microsomal fraction was prepared from the post-mitochondrial supernatant by centrifugation at 104,000 × g for 1 h. For small scale incubations (0.5 ml), microsomes (5 mg/ml) were incubated with 100 μM 7DHP (added from a 2.5 mM ethanol stock) in buffer comprising 20 mM HEPES (pH 7.4), 100 mM NaCl, 0.1 mM dithiothreitol, 0.1 mM EDTA and 0.4 mM NAD^+, for 10 min at 37°C. Reactions were stopped by the addition of 2.5 ml ice-cold methylene chloride and extracted as described for the incubations with mitochondria. Samples were analysed by HPLC using a Grace Alltima C18 column (25 cm × 4.6 mm) with a mobile phase of 64% methanol in water for 5 min followed by a gradient of 64–100% methanol in water for 25 min, then 100% methanol for 40 min, at 0.5 mL/min, with a UV monitor set to 250 nm. For large scale incubations to isolate product for NMR analysis, the incubation was scaled up to 30 ml. Following HPLC as above, the major product (shown to be 7-dehydroprogesterone, see Results) was further purified on the same column using a mobile phase of 45% acetonitrile in water for 5 min followed by a gradient of 45–100% acetonitrile in water for 45 min then 100% acetonitrile for 15 min, at 0.5 mL/ min. The concentration of 7-dehydroprogesterone was measured in ethanol at 238 nm using the extinction coefficient of 14,600 M^{-1} cm^{-1} (Dorfman, 1953). The large scale procedure yielded 135 μg of 7-dehydroprogesterone of which 100 μg was used for NMR analysis.

2.7. NMR spectroscopy

NMR measurements were performed using an inverse triple-resonance 3 mm probe on a Varian Unity Inova 500 MHz spectrometer running VNMRJ 2.2D (Agilent Technologies, Inc., Santa Clara, CA, U.S.A.). Sample was dissolved in CD_3OD and transferred to a 3-mm Shigemi NMR tube (Shigemi Inc., Allison Park, PA). Temperature was regulated at 22°C and was controlled with an accuracy of ± 0.1°C. Chemical shifts were referenced to residual solvent peaks for CD_3OD (3.31 ppm for proton and 49.15 ppm for carbon). Standard two-dimensional NMR experiments [(^{1}H-^{1}H correlation spectroscopy (COSY), ^{1}H-^{1}H total correlation spectroscopy (TOCSY), ^{1}H-^{13}C heteronuclear single quantum correlation spectroscopy (HSQC), and ^{1}H-^{13}C heteronuclear multiple bond correlation spectroscopy (HMBC)] were acquired in order to fully elucidate the structures of the metabolites. All data were transferred from the spectrometer to an offline PC data-station and processed using ACD software version 12.0 (Advanced Chemistry Development, Toronto, ON, Canada), with zero-filling in the direct dimension and linear prediction in the indirect dimension.

2.8. Experiments with epidermal keratinocytes

2.8.1. Metabolism of 7DHC by epidermal keratinocytes—The detailed protocols for experiments with keratinocytes are described in (Slominski et al., 2012a). Briefly, the pig epidermal keratinocytes were isolated from the skin of 2 year old, female, white pigs bred at Nicole farm in Memphis, TN and killed at the animal care unit of the UTHSC, following protocols used to isolate human primary keratinocytes (Janjetovic et al., 2010). We also used human immortalized (HaCaT) keratinocytes that are maintained in culture in our laboratory (Zbytek et al., 2008). Suspensions of human or pig skin keratinocytes were incubated with or without 50 μM 7DHC in tris-buffered medium (110 mM NaCl, 5 mM KCl, 2.5 mM $CaCl_2$, 1 mM $MgSO_4$, 1 mM KH_2PO_4, 33 mM Tris-HCl, pH7.4) containing 5 mM isocitrate, 0.5 mM NADPH and 0.2% glucose, for 16 h. The incubation mixtures were then extracted with dichloromethane, re-dissolved in methanol and products separated by HPLC with a gradient of methanol in water (85–100%) for 20 min and 100% methanol for 10 min,

at flow rate of 0.5 ml/min with UV detector set at 280 nm. The extracts were also analyzed by an API-3000 LC-MS/MS (see above) with separations performed isocratically using 96% methanol in water at a flow rate of 0.05 ml/min for 35 min on a Zorbax Eclipse Plus C18 column (see above).

2.8.2. Cell proliferation assay—HaCaT keratinocytes were plated in 96-welll plates, 5,000 cells/well in DMEM + 5% FBS. After overnight incubation, media were replaced with fresh media containing 5% charcoal-stripped serum and diluted compounds: 7DHP or pD, at concentrations ranging from 0.1–100 nM. EtOH served as a vehicle. After 68 h of incubation, MTT (Promega) was added to the cells, 20 μl/ well, at a concentration of 5 mg/ ml. After 4 h of incubation supernatant was removed and cells were solubilized in Isopropranol/ 0.1 N HCl solution, 100 μl/well, for 20 min with shaking at room temperature. Absorbance was measured at 570 nm.

2.9. Molecular Modeling of 7DHC and cholesterol interaction with P450scc

We conducted molecular modeling studies using the crystal structure of human P450scc in complex with 20R,22R-dihydroxycholesterol (Protein Data Bank code 3NA0) (Strushkevich et al., 2011) and using Schrodinger Molecular Modeling Suite 2011 (Schrodinger Inc., Portland, OR) following similar procedures to those described previously (Chen et al., 2011, Chen et al., 2010). Briefly, we used the Protein preparation wizard and defined the active site by the Glide grid generation module. Molecules were built and prepared using the Ligprep module, and they were docked into the active site of P450scc using the Glide ligand docking module in Schrodinger Suite.

3. Results and Discussion

3.1. Metabolism of 7DHC by purified human P450scc

Previously we have shown that the rat adrenal gland can convert 7DHC to 7DHP in a reaction attributed to P450scc, wherein there is an accumulation of the intermediates 22(OH)7DHC and 20,22(OH)$_2$7DHC (Slominski et al., 2009). We have also shown that 7DHC is a better substrate (higher k_{cat}/K_m) than cholesterol for human P450scc using a procedure involving radioimmunoassay of the 7DHP product (Slominski et al., 2009). Since P450scc is the enzyme in the human placenta that is likely to metabolize 7DHC, initially we examined the ability of purified human cytochrome P450scc to metabolize 7DHC using HPLC analysis to look for the production of reaction intermediates. Following incubation of 7DHC with purified human P450scc, 7DHP was seen as the major product (Fig. 1). Five other products were also observed with retention times between those of 7DHC and 7DHP (Fig. 1), with each representing more than 2% of the total products. Most notable was product (P) 2 which represented 7.5% of the total products. All these products were present at concentrations greater than 4 × the P450scc concentration, indicating that they can be considered as true products of the reaction and are not just enzyme-bound intermediates. To permit further metabolite analysis, a 75 ml incubation of purified human P450scc with 7DHC was conducted and products 2–5 were collected following their HPLC separation. This yielded 330 nmol of product 2 and 30–60 nmol of products 3–5. All of these products had a similar UV spectrum to 7DHC indicating that the 5,7-diene motif remained intact. To test whether products 2–5 were intermediates in the conversion of 7DHC to 7DHP, they were incubated with purified human P450scc in a phospholipid vesicle reconstituted system. Concentrations of substrate were low (0.025 mol sterol/mol phospholipid), due to the limited availability of these compounds. P4 was not metabolized further by P450scc (not shown). P2 was metabolized to a product identified as 7DHP (Fig. 2A) from its retention time and spiking with authentic standard. P3 was almost completely consumed by the P450scc, with metabolite peaks corresponding to P2 and 7DHP being observed (Fig. 2B). P5 was slowly

metabolized giving a final product corresponding in retention time to 7DHP. Mass spectral analysis of P2 showed the major ion at 439.3 $[M + Na]^+$ corresponding to a true mass of 416.3, indicating that it is a dihydroxy-derivative of 7DHC (Fig. 3A). Mass spectrometry analysis identified ions 401 $[M + 1]^+$ and 383 $[M + 1- H_2O]^+$ for products 3 and 4 and ions 383 $[M + 1-H_2O]^+$ and 365 $[M + 1-H_2O]^+$ for P5 indicating that these are monohydroxy-derivatives. The data clearly indicate that P3 is an intermediate in the conversion of 7DHC to 7DHP with initial conversion to P2, the dihydroxy-intermediate, before the cleavage of the side chain. The likely identity of P2 is $20,22(OH)_2$7DHC since there is production of a similar dihydroxy-intermediate in the conversion of 7DHC to 7DHP in the rat adrenal gland (Slominski et al., 2009) and 20,22-dihydroxycholesterol is well characterized as the second intermediate in the conversion of cholesterol to pregnenolone (Hume et al., 1984, Miller and Auchus, 2011, Tuckey, 2005, Tuckey and Cameron, 1993b). This prediction was confirmed by NMR analysis performed on 330 nmol of this product, as described in the next section. We were able to demonstrate that none of the monohydroxy-derivatives (P3, P4 or P5) were 20S(OH)7DHC, since HPLC analysis of chemically synthesized 20*S*(OH)D3 showed that it had a retention time between P4 and P5, confirmed by spiking of the P450scc reaction extract. This indicates that the conversion of 7DHC to $20,22(OH)_2$7DHC proceeds through the 22(OH)7DHC intermediate. Furthermore, this intermediate is most likely to be P3 since this is rapidly converted to 7DHP and it has a shorter retention time than 20*S*(OH)7DHC as would be predicted from the relative retention time of the closely related 20 and 22-hydroxy-derivatives of cholesterol and vitamin D3. The identities of P4 and P5 remain to be established, but they may be monohydroxy-derivatives of 7DHC with the site of hydroxylation further among the side chain, such as at C23, a known site of vitamin D3 hydroxylation by P450scc (Tuckey et al., 2008a).

To obtain further support for the above hydroxylation pattern of 7DHC in its conversion to 7DHP, we modeled the substrate and intermediates into the active site of P450scc using the crystal structure of human P450scc bound to 20R,22Rdihydroxycholesteol. Modeling of 7DHC into the active site (Supplemental Fig. S-7) revealed that the one of the C22 hydrogens was closer (2.9 Å) to the heme iron than the hydrogen at C20 (3.2 Å), consistent with initial hydrogen abstraction and hence hydroxylation being favored at C22, as suggested by the experimental evidence presented above. Docking scores were highest (indicating tightest binding) for the 22-hydroxyderivatives of both 7DHC and cholesterol, with the 20,22-dihydroxyderivatives having intermediate docking scores, higher than for cholesterol or 7DHC (Supplemental Fig. S-8). This pattern is consistent with the known relative binding strengths for cholesterol and its intermediates (Strushkevich et al., 2011, Tuckey and Cameron, 1993a). 7DHC and its intermediates showed slightly higher docking scores than cholesterol and its corresponding intermediates.

3.2. Determination of the structure of the dihydroxy-7DHC (Product 2) as $20,22(OH)_2$7DHC

The sites of hydroxylation were unambiguously assigned to be at C-20 and C-22 based on the NMR spectra for this metabolite and mass spectrometry (Fig. 3, Table 1, Supplemental Figs. S-1-S-6). First, we assigned the hydroxylation at C-20. The doublet of $21-CH_3$ in 7DHC became a singlet in the metabolite (^{1}H at 1.20 p.p.m, ^{13}C at 20.8 p.p.m, Figs 3B and 3C), indicating the loss of scalar coupling from 20-CH. All five methyl groups (18, 19, 21, 26, 27) are intact [Fig. 3C projection]. From 1H-^{13}C HMBC, $21-CH_3$ (^{1}H at 1.20 p.p.m) has correlations to C-17 at 55.9 p.p.m and C-20 at 77.7 p.p.m (Fig. 3D), implying that the 20-C is connected with a hydroxyl group. Thus, the presence of a 20-OH group in the metabolite is unambiguously established. Second, we assigned hydroxylation at 22-C based on the following rationale. ^{1}H-NMR and ^{1}H-^{13}C HSQC revealed a new methine peak at 3.32 p.p.m (^{13}C at 77.6 p.p.m, Fig. 3C, insert) which is characteristic for a methine connected directly to an oxygen atom. From ^{1}H-^{1}H TOCSY (Fig.3E), this methine at 3.32 p.p.m has

correlations to 26/27-CH$_3$ (0.92/0.91 p.p.m), suggesting that this methine is in the same spin system as 26/27-CH$_3$. Therefore the hydroxylation occurred in the side chain. From ^{1}H-^{13}C HMBC, 21-CH$_3$ (1.20 p.p.m) showed only two correlations to C-17 at 55.9 p.p.m and C-20 at 77.7 p.p.m (Fig. 3D). If 22-CH$_2$ were not hydroxylated, 21-CH$_3$ would have correlation to 22-C at 30–45 p.p.m. Since the newly identified methine is at 77.6 p.p.m and is the same as 20-C (^{13}C at 77.7 p.p.m), the only rationale for the missing correlation from 21-CH$_3$ to 22-C at 30–45 p.p.m is that 22-CH$_2$ is hydroxylated, and the ^{13}C chemical shift for 22-C (77.6 p.p.m) is coincidently overlapping with 20-C (77.7 p.p.m) in the ^{1}H-^{13}C HMBC spectrum which has limited resolution in the ^{13}C dimension. This is consistent with our previous reports for 20,22-dihydroxyvitamin D$_3$ in which the 20-C and 22-C had similar carbon chemical shift (Janjetovic et al., 2011). Thus, the second hydroxylation site was assigned to be at the 22-position, as could be further confirmed by the ^{1}H-^{1}H COSY in which 22-CH (3.32 p.p.m) showed the expected vicinal coupling to the 23-CH$_2$ (1.50/1.22 p.p.m, Fig. 3F). Collectively the structure of this metabolite was determined to be 20,22(OH)$_2$7DHC. The full assignments for this metabolite are summarized in Table 1, and full spectra for all 1D/ 2D NMR are shown in supplementary materials (Supplemental Fig. S-2-S-6). While the stereochemistry at C-20 and C-22 remain to be established, it is highly likely that the it is 20*R*,22*R*-dihydroxy-7-dehydrocholesterol, by analogy to 20*R*,22*R*-dihydroxycholesterol, the second intermediate in the conversion of cholesterol to pregnenolone by P450scc (Hume et al., 1984, Miller and Auchus, 2011, Tuckey, 2005). This is supported by the modeling of 7DHC into the active site of P450scc (Supplemental Fig. S-7) where alignment of the side chain of 7DHC relative to the heme group is similar to that for cholesterol.

3.3. Metabolism of 7DHC by placental mitochondria

The ability of placental mitochondria to convert 7DHC to 7DHP was tested in the presence of the N-62 StAR protein to facilitate 7DHC transport (Tuckey et al., 2004), and cyanoketone to block the action of 3β-hydroxysteroid dehydrogenase (Arthur and Boyd, 1974). HPLC analysis revealed the formation of one major product, in 20% yield (Fig. 4). This was identified as 7DHP from its UV spectrum (the same as that for the parent 7DHC) and its identical retention time to authentic 7DHP standard. Importantly, 22R-hydroxycholesterol almost completely inhibited the metabolism of 7DHC. Since 22R-hydroxycholesterol binds tightly to P450scc and displays a very low K$_m$ for its metabolism to pregnenolone (Tuckey and Cameron, 1993a, Woods et al., 1998), it acts efficiently as a competitive substrate with the 7DHC (Fig. 4). This provides proof that placental production of 7DHP is a P450scc mediated reaction, similar to what has been reported for adrenal gland (Slominski et al., 2009). Minor products were also observed in the incubations with placental mitochondria, with retention times in between those of the 7DHC substrate and 7DHP. As for the studies described above for purified P450scc, some of these likely represent reaction intermediates with one of the major ones having an identical HPLC retention time and UV spectra to 20,22(OH)$_2$7DHC (Figs 1, 2).

We compared the ability of placental mitochondria to metabolize exogenous 7DHC (200 μM) with their ability to metabolize an equal concentration of exogenous [4-^{14}C]cholesterol in both the presence and absence of the N-62 StAR protein (Fig. 5). [4-^{14}C]cholesterol (200 μM) was used to measure the metabolism of the exogenous cholesterol, separately from the abundant endogenous cholesterol present in placental mitochondria (Tuckey et al., 2004). Under the assay conditions used both 7DHC and the exogenous [4-^{14}C]cholesterol compete with the endogenous cholesterol for metabolism by P450scc. Time courses for the metabolism of both 7DHC and exogenous [4-^{14}C]cholesterol were linear for the duration of the 2 h incubation. In the absence or presence of StAR protein, 7DHC was converted to 7DHP at 1.75 and 1.64 fold faster, respectively, than for exogenous [4-^{14}C]cholesterol conversion to [4-^{14}C]pregnenolone (Fig. 5). The N-62 StAR protein stimulated the

metabolism of both [4-^{14}C]cholesterol and 7DHC approximately 7.5 fold. It should be noted that in the absence of the N-62 StAR protein, the rate of side-chain cleavage is determined both by delivery of exogenous cholesterol to the P450scc in the inner mitochondrial membrane and by the size of the endogenous cholesterol pool. While MLN64 and not the StAR protein appears to be the cholesterol transfer protein found in placental mitochondria, the proteins are closely related and act similarly (Tuckey, 2005, Tuckey et al., 2004, Bose et al., 2000). The StAR protein can rapidly transfer cholesterol to the inner mitochondrial-membrane site of P450scc action in isolated mitochondria (Tuckey et al., 2004). We have also previously shown that the StAR protein can transfer 7DHC between membranes with a similar efficiency to cholesterol transfer (Slominski et al., 2009). With the 5 μM StAR concentration used for Fig. 5, the sterol transfer rate is at a maximum and the activity of the P450scc itself limits the rate of side chain cleavage (Tuckey et al., 2004). It is thus evident from Fig. 5 that exogenous 7DHC is metabolized at a faster rate than an equivalent concentration of exogenous cholesterol, under both limiting and saturating conditions of substrate transport. The latter is consistent with our previous report using human P450scc in a phospholipid-vesicle-reconstituted system where the enzyme displayed a slightly higher catalytic efficiency (k_{cat}/K_m) with 7DHC as substrate than with cholesterol (Slominski et al., 2009, Slominski et al., 2004).

3.4. Metabolism of 7DHC by placental fragments ex-utero

To test the ability of intact placenta to metabolize exogenously added 7DHC we cut the placental tissue obtained shortly after the delivery (to mimic the in vivo conditions) and incubated it with exogenously added substrates. Incubation of placental fragments with 7DHC resulted in the formation of 7DHP as identified from its identical retention time to authentic standard and from its mass spectrum which showed m/z = 315 for [M + 1]$^+$ (molecular weight of 314). The mass spectral analysis was done by LC/MS using both total ion scanning (LC/MS-TIC) and selective ion monitoring (LC/MS SIM) modes (Fig. 6). The 7DHP product was absent in negative controls incubated either without substrate or after boiling of placental fragments. Formation of 7DHP was rapid with this metabolite being detected at 3 h of incubation in a manner dependent on both the amount of added tissue and the concentration of the substrate (Fig. 7). 7DHP product was detected at concentration as low as 10 μM 7DHC (Fig. 7). The nature of an additional product with m/z = 315 for [M + 1]$^+$ could not be determined because of a lack of proper standard and insufficient material for NMR analysis (Fig. 7A). The placental production of 7DHP was inhibited by addition of 200 μM DL-aminoglutethimide (AGT) (Fig. 8), indicating the involvement of P450scc (plus see below). It was also stimulated by 100 μM forskolin which suggest the involvement of the cAMP-dependent pathway in this metabolism (Tuckey, 2005). The conclusive evidence for P450scc involvement was provided in isolated placental mitochondria where production of 7DHP was almost completely inhibited by 22R-hydroxycholesterol (see Fig. 4). Thus, we show for the first time that the human placenta transforms 7DHC to 7DHP. The regulatory mechanisms are apparently similar to those observed in adrenal glands incubated ex-vivo (Slominski et al., 2009).

To determine whether accumulation of intermediates in the conversion of 7DHC to 7DHP occurs in placental fragments we used a photodiode array detector to detect all 5,7-dienal products. Five 5,7-dienal metabolites with identical UV spectra (UV λmax 261, 271, 281, 293) to 7DHC and polarity between 7DHC and 7DHP were detected in the chromatogram of the extract from placental fragments incubated with 7DHC (Fig. 9). These metabolites (fractions 1–5) were absent in control incubations without substrates or with substrate incubated with boiled tissue (Fig. 9B). Fractions 1–5 were collected and subjected to LC/MS analysis. Metabolite 1 was identified as a dihydroxy-7DHC from its mass spectrum (Fig. 9C). Based on its mass and a retention time identical to P2 that was defined as

20,22(OH)$_2$7DHC by NMR studies (see above), this product most likely represents 20,22(OH)$_2$7DHC.The mass spectrum of the 5,7-dienal metabolite 2 (Fig. 9C) and its identical retention time to P3 (Fig 1) indicates that it represents 22(OH)7DHC, since it is converted by P450scc to 20,22(OH)$_2$7DHC and 7DHP (Fig. 2B). Similar intermediate was detected in the conversion of 7DHC to 7DHP in adrenal glands (Slominski et al., 2009). A metabolite 3 corresponding to the retention time of P4 had a major ion at m/z = 401 [corresponding to [M + 1]$^+$] and a minor ion at m/z = 383 [corresponding to [M + 1 - H$_2$O]$^+$] indicating that it represents a 7DHC hydroxyderivative. Since it had a retention time different from either 20S or 20R(OH)7DHC or 22(OH)7DHC, and there was insufficient material to perform the NMR analysis necessary to define the position of the hydroxyl group, we tentatively defined this product as (OH)7DHC. Metabolite 4 showed a major ion at m/z = 383 [corresponding to [M + 1 – H$_2$O]$^+$, indicating that it represents a monohydroxy-7DHC ((OH)7DHC). Also it had an identical retention time to P5 (as defined by spiking with P5 standard). Finally, due to the very limited amount of the sample collected, we were unable to identify the 5,7-diene corresponding to metabolite 5, which had a retention time close but different from the parent 7DHC.

3.5. Metabolism of 7DHP by human placentas

Placental microsomes converted 7DHP to a single major product in a 10 min incubation (Fig. 10) with most of the 7DHC substrate being consumed. Some endogenous progesterone, also present in the control incubation, was also seen in the chromatogram, identified from its absorbance maximum at 241 nm (Dorfman, 1953) and by its identical retention time to authentic standard.

Since the metabolism of 7DHP by placental microsomes was completely blocked by cyanoketone (Fig. 10) a specific 3β-hydroxysteroid dehydrogenase (3β-HSD) inhibitor (Bose et al., 2000), metabolism can be attributed to the action of this enzyme. Thus by analogy to the action of this enzyme in converting pregnenolone to progesterone, the expected product from 7DHP was 7-dehydroprogesterone. The UV spectrum which showed a peak at 237 nm (Fig. 10), is consistent with the literature for 7- dehydroprogesterone (peak at 238 nm) (Djerassi et al., 1951, Dorfman, 1953). However, we observed that on storage for a few hours at room temperature, the putative 7-dehydroprogesterone rapidly attained a yellowish appearance with a broad absorption extending into the visible region with a peak at 339 nm (Fig. 10). This was coupled to the appearance of impurities in the HPLC chromatogram, indicating that 7- dehydroprogesterone is unstable. No information on the stability of 7- dehydroprogesterone was provided in the one reference reporting its chemical synthesis in 1951 (Djerassi et al., 1951).

The structure of 7-dehydroprogesterone was further confirmed by NMR and mass spectroscopy. First, mass spectrometry (Fig. 11A) carried out immediately after sample purification identified the molecular ion of 335 [M + Na]$^+$ which is consistent with the proposed structure of 7-dehydroprogesterone (MW=312). Second, from 1H NMR (Fig. 11B) spectroscopy, we can clearly see the presence of two double bond protons at 5.8 and 5.3 p.p.m, which could be assigned to 4-CH and 7-CH, respectively. Consistent with this assignment, 1H-1H COSY (Fig. 11C) showed the expected correlations from 7-CH (1H at 5.3 p.p.m) to 6-CH2 (1H at 3.2 and 2.7 p.p.m), and from 4-CH (1H at 5.8 p.p.m) to one of the 6-CH2 protons at 3.2 p.p.m. Furthermore, from 1H-1H TOCSY (Fig. 11D), the correlations from 7-CH (1H at 5.3 p.p.m) to 6-CH2 (1H at 3.2 and 2.7 p.p.m) can be identified. Because of the instability and very limited amount of this compound, we were unable to acquire usable 1H-13C HSQC and 1H-13C HMBC spectra which is necessary for fully elucidating the structure. However, taken together the abovementioned analysis, we assign the structure of this product as 7-dehydroprogesterone.

Most importantly, we investigated whether the 7DHP product could be further metabolized by human placenta ex-utero. Human placental fragments were incubated with 7DHP and after extraction were subjected to HPLC analysis which revealed a product with a UV maximum at 238 nm with the mass spectrum showing m/z=313 and 295 for [M+1]$^+$ and [M+1-H$_2$O]$^+$, respectively, and a retention time identical to the 7- dehydroprogesterone standard identified by NMR (Fig. 12A). This product was absent in control incubations with boiled placenta or fresh placenta incubated without the addition of substrate (Fig. 12B, C). The above data indicate that human placenta in vivo can metabolize 7DHP to 7-dehydroprogesterone.

Additional analysis of incubations with placental fragments showed a small peak with UV spectra characteristic of a 5,7-diene (λmax 261, 271, 281 and 293 nm) with m/z=317 and 339 for [M+1]$^+$ and [M+Na]$^+$, respectively (Fig. 12D). This product was absent in control incubations with boiled placenta or placenta without a substrate (Fig. 12E, F). Since 20α-hydroxysteroid dehydrogenase (20α-HSD) is expressed in the placenta (Ma and Penning, 1999) we suggest that the species with real mass of 316 may represent 20(OH)7DHP (5,7-pregnadiene-3β,20-diol). In summary, our data on 7DHP metabolism by placenta indicates that it is predominantly converted to 7- dehydroprogesterone with minor production of 5,7-pregnadien-hydroxyderivative of whose definitive structure remains to be confirmed by NMR.

3.6. Metabolism of 7DHC by epidermal keratinocytes

Since the skin express low levels of P450scc but sufficient to initiate local steroidogenesis (Slominski et al., 2004, Slominski et al., 1996, Slominski et al., 2012b), and the epidermis is the major source of 7DHC, the precursor to vitamin D3 (Holick, 2003, Bikle, 2011), we tested whether epidermal keratinocytes can transform 7DHC to 7DHP. In the first step we incubated immortalized human HaCaT keratinocytes with exogenously added 7DHC (50 μM) and analyzed its metabolism (Supplemental Fig. S-9). LCMS analysis in the SIM mode showed the presence of compounds with both masses and retention times corresponding to 7DHP, 22(OH)7DHC and 20,22(OH)$_2$7DHC, which were below the detectability limit by HPLC with UV detection, indicating a low level of production (Supplemental Fig. S9). Next, we used epidermal keratinocytes isolated from pig skin containing high levels of endogenous 7DHC detectable on UV monitoring (Fig. 13). LC-MS/MS analysis in the MRM mode showed the characteristic transition (m/z = 315[M+1]$^+$ → 297[M+1-H$_2$O]$^+$) at the correct retention time of the 7DHP standard, confirming that the product was endogenously produced 7DHP (Fig. 13A). In addition, the expected ions for dihydroxy (m/z = 417[M+1]$^+$) and monohydroxy7DHC (m/z = 401[M+1]$^+$) were detected in the SIM mode at the proper retention time for 20,22(OH)$_2$7DHC and 22(OH)7DHC (Fig. 13A). These results clearly demonstrate that epidermal keratinocytes can transform 7DHC to 22(OH)7DHC, 20,22(OH)$_2$7DHC and 7DHP. We also performed preliminary assessment of the anti-proliferative activity of 7DHP using the MTT test and showed that it inhibited proliferation of cultured keratinocytes in a dose-dependent manner (Fig. 13B). This effect disappeared when pregnacalciferol (pD), produced from UVB-induced B-ring opening of 7DHP, was analysed (Fig. 13C)(Zmijewski et al., 2008).

4. Concluding remarks and perspectives

In summary, we demonstrate for the first time that the human placenta, which expresses relatively high levels of P450scc, can metabolize, in vivo, exogenously added 7DHC to 7DHP, and an exogenously added 7DHP to 7-dehydroprogesterone and a monohydroxy-7DHP (most likely 20(OH)7DHP). Using chemically synthesized standards, the enzymatic properties of purified human cytochrome P450scc, and NMR, MS and UV spectrometric analyses we were able to identify the two major intermediates of the pathway

of 7DHC metabolism to 7DHP as 22(OH)7DHC and 20,22(OH)$_2$7DHC. Other minor monohydroxy-7DHC metabolites that we were not able to fully identify were also produced. Furthermore, the human placenta ex-utero as well as the microsomal fraction of the placenta transformed 7DHP to 7-dehydroprogesterone (Figs 10–12). Thus 7DHC is converted to 7DHP by the same reaction sequence as that reported for the conversion of cholesterol to pregnenolone by P450scc, with initial hydroxylation at C22 being favoured (Tuckey, 2005, Hume et al., 1984). The difference between 7DHC and cholesterol metabolism is that there is appreciable accumulation of reaction intermediates and other hydroxy-7DHC derivatives only for 7DHC metabolism. In contrast to cholesterol and 7DHC metabolism, initial hydroxylation of vitamin D3 by P450scc strongly favors C20, which modeling shows is closer to the haem iron than C22, due to the extended conformation of this molecule associated with its open B-ring structure (Strushkevich et al., 2011). The minor monohydroxy-7DHP products of 7DHP metabolism may represent 20(OH)7DHP, since 20α-HSD is expressed in the placenta (Ma and Penning, 1999). We also tested epidermal keratinocytes that express P450scc only at a low level and found that they can transform both exogenous and endogenous 7DHC to 7DHP with production of 22(OH)7DHC and 20,22(OH)$_2$7DHC as intermediates. Therefore, we propose that in vivo metabolism of 7DHC is similar in tissues expressing high (human placenta) and low (epidermal keratinocytes) levels of P450scc, following the sequence 7DHC →22(OH)7DHC → 20,22(OH)$_2$7DHC → 7DHP→ 7-dehydroprogesterone and/or hydroxy7DHP (Fig. 14). The possibility of metabolism of 7DHP to 7-dehydroprogesterone in keratinocytes is supported by the presence of 3βHSD in the skin, while hydroxylations of 7DHP is supported by presence of steroidogenic enzymes in this tissue (Slominski et al., 2012b).

These pathways are substantiated by the in vivo metabolism of 7DHC to 7DHP in horses during synthesis of equilin (Tait et al., 1983) and by the accumulation of 5,7- dienal products in SLOS (Nowaczyk and Waye, 2001, Tint et al., 1994, Shackleton et al., 1999). Their pathological consequences are exemplified by contributions of 5,7- dienes to the phenotypic presentation of SLOS patients (Nowaczyk and Waye, 2001, Tint et al., 1994, Shackleton et al., 1999). An example of the physiological significance of the pathway is the inhibition of keratinocyte proliferation caused by 7DHP. It must be noted that hydroxyderivatives of 7DHP or the products of their phototransformation show anti-proliferative activity against melanoma and leukemia cells cultured in vitro (Slominski et al., 2009, Zmijewski et al., 2009, Kim et al., 2010, Zmijewski et al., 2011, Slominski et al., 2010), suggesting their potential therapeutic utility. In fact, therapeutic utilities for novel hydroxyl-derivatives of vitamin D, acting through the vitamin D receptor, have already been demonstrated (Janjetovic et al., 2009, Zbytek et al., 2008, Janjetovic et al., 2010, Slominski et al., 2010, Zmijewski et al., 2009, Slominski et al., 2011b, Slominski et al., 2011a, Slominski et al., 2006). Lastly, it is theoretically possible that hydroxyl-dervatives of 7DHC can act as ligands for the nuclear receptor LXRα, since oxysterols including 20(OH)cholesterol, 22(OH)cholesterol and 20,22(OH)$_2$cholesterol can act as ligands for this orphan receptor (Janowski et al., 1996, Ruan et al., 1999). Thus, our findings that tissues expressing P450scc can metabolize 7DHC to biologically active 7DHP not only open new possibilities in biochemistry but also have profound physiological and pharmacological implications in general.

Supplementary Material

Refer to Web version on PubMed Central for supplementary material.

Acknowledgments

Abbreviations

cyclodextrin	2-hydroxypropyl-ß-cyclodextrin
COSY	correlation spectroscopy
7DHP	7-dehydropregnenolone
7DHC	7-dehydrocholesterol
HSQC	heteronuclear single quantum correlation
HMBC	heteronuclear multiple bond correlation
pD	pregcalciferol
TOCSY	total correlation spectroscopy
RT	retention time

References

Arthur JR, Boyd GS. The effect of inhibitors of protein synthesis on cholesterol side-chain cleavage in the mitochondria of luteinized rat ovaries. Eur J Biochem. 1974; 49:117–127. [PubMed: 4459139]

Bikle DD. Vitamin D: an ancient hormone. Exp Dermatol. 2011; 20:7–13. [PubMed: 21197695]

Bose HS, Baldwin MA, Miller WL. Evidence that StAR and MLN64 act on the outer mitochondrial membrane as molten globules. Endocrine research. 2000; 26:629–637. [PubMed: 11196440]

Chen J, Li CM, Wang J, Ahn S, Wang Z, Lu Y, Dalton JT, Miller DD, Li W. Synthesis and antiproliferative activity of novel 2-aryl-4-benzoyl-imidazole derivatives targeting tubulin polymerization. Bioorg Med Chem. 2011; 19:4782–4795. [PubMed: 21775150]

Chen J, Wang Z, Li CM, Lu Y, Vaddady PK, Meibohm B, Dalton JT, Miller DD, Li W. Discovery of novel 2-aryl-4-benzoyl-imidazoles targeting the colchicines binding site in tubulin as potential anticancer agents. J Med Chem. 2010; 53:7414–7427. [PubMed: 20919720]

Djerassi C, Romo J, Rosenkranz G. Steroidal sapogenins. VIII. Steroids. XVIII. Synthesis of Δ7,9(11)-allopregnadien-3β-ol-20-one from diosgenin and from Δ5-pregnen-3β-ol-20-one. The Journal of Organic Chemistry. 1951; 16:754–760.

Dorfman L. Ultraviolet absorption of steroids. Chem Rev. 1953; 53:47–144.

Guryev O, Carvalho RA, Usanov S, Gilep A, Estabrook RW. A pathway for the metabolism of vitamin D3: unique hydroxylated metabolites formed during catalysis with cytochrome P450scc (CYP11A1). Proc Natl Acad Sci U S A. 2003; 100:14754–14759. [PubMed: 14657394]

Holick MF. Vitamin D: A millenium perspective. J Cell Biochem. 2003; 88:296–307. [PubMed: 12520530]

Hume R, Kelly RW, Taylor PL, Boyd GS. The catalytic cycle of cytochrome P-450scc and intermediates in the conversion of cholesterol to pregnenolone. Eur J Biochem. 1984; 140:583–591. [PubMed: 6723652]

Janjetovic Z, Brozyna AA, Tuckey RC, Kim TK, Nguyen MN, Jozwicki W, Pfeffer SR, Pfeffer LM, Slominski AT. High basal NF-kappaB activity in nonpigmented melanoma cells is associated with an enhanced sensitivity to vitamin D3 derivatives. Br J Cancer. 2011; 105:1874–1884. [PubMed: 22095230]

Janjetovic Z, Tuckey RC, Nguyen MN, Thorpe EM Jr, Slominski AT. 20,23-dihydroxyvitamin D3, novel P450scc product, stimulates differentiation and inhibits proliferation and NF-kappaB activity in human keratinocytes. J Cell Physiol. 2010; 223:36–48. [PubMed: 20020487]

Janjetovic Z, Zmijewski MA, Tuckey RC, DeLeon DA, Nguyen MN, Pfeffer LM, Slominski AT. 20-Hydroxycholecalciferol, product of vitamin D3 hydroxylation by P450scc, decreases NF-kappaB activity by increasing IkappaB alpha levels in human keratinocytes. PLoS One. 2009; 4:e5988. [PubMed: 19543524]

Janowski BA, Willy PJ, Devi TR, Falck JR, Mangelsdorf DJ. An oxysterol signalling pathway mediated by the nuclear receptor LXR alpha. Nature. 1996; 383:728–731. [PubMed: 8878485]

Kim TK, Chen J, Li W, Zjawiony J, Miller D, Janjetovic Z, Tuckey RC, Slominski A. A new steroidal 5,7-diene derivative, 3beta-hydroxyandrosta-5,7-diene-17beta-carboxylic acid, shows potent anti-proliferative activity. Steroids. 2010; 75:230–239. [PubMed: 20025893]

Ma H, Penning TM. Conversion of mammalian 3alpha-hydroxysteroid dehydrogenase to 20alpha-hydroxysteroid dehydrogenase using loop chimeras: changing specificity from androgens to progestins. Proc Natl Acad Sci U S A. 1999; 96:11161–11166. [PubMed: 10500147]

Marcos J, Guo LW, Wilson WK, Porter FD, Shackleton C. The implications of 7-dehydrosterol-7-reductase deficiency (Smith-Lemli-Opitz syndrome) to neurosteroid production. Steroids. 2004; 69:51–60. [PubMed: 14715377]

Miller WL, Auchus RJ. The molecular biology, biochemistry, and physiology of human steroidogenesis and its disorders. Endocrine reviews. 2011; 32:81–151. [PubMed: 21051590]

Nguyen MN, Slominski A, Li W, Ng YR, Tuckey RC. Metabolism of vitamin d2 to 17,20,24-trihydroxyvitamin d2 by cytochrome p450scc (CYP11A1). Drug metabolism and disposition: the biological fate of chemicals. 2009; 37:761–767. [PubMed: 19116262]

Nowaczyk MJ, Waye JS. The Smith-Lemli-Opitz syndrome: a novel metabolic way of understanding developmental biology, embryogenesis, and dysmorphology. Clin Genet. 2001; 59:375–386. [PubMed: 11453964]

Ruan B, Wilson WK, Schroepfer GJ Jr. An improved synthesis of (20R,22R)-cholest-5-ene-3beta, 20,22-triol, an intermediate in steroid hormone formation and an activator of nuclear orphan receptor LXR alpha. Steroids. 1999; 64:385–395. [PubMed: 10433175]

Shackleton C, Roitman E, Guo LW, Wilson WK, Porter FD. Identification of 7(8) and 8(9) unsaturated adrenal steroid metabolites produced by patients with 7-dehydrosterol-delta7-reductase deficiency (Smith-Lemli-Opitz syndrome). J Steroid Biochem Mol Biol. 2002; 82:225–232. [PubMed: 12477489]

Shackleton CH, Roitman E, Kelley R. Neonatal urinary steroids in Smith-Lemli-Opitz syndrome associated with 7-dehydrocholesterol reductase deficiency. Steroids. 1999; 64:481–490. [PubMed: 10443904]

Slominski A, Ermak G, Mihm M. ACTH receptor, CYP11A1, CYP17 and CYP21A2 genes are expressed in skin. J Clin Endocrinol Metab. 1996; 81:2746–2749. [PubMed: 8675607]

Slominski A, Semak I, Wortsman J, Zjawiony J, Li W, Zbytek B, Tuckey RC. An alternative pathway of vitamin D metabolism. Cytochrome P450scc (CYP11A1)-mediated conversion to 20-hydroxyvitamin D2 and 17,20-dihydroxyvitamin D2. FEBS J. 2006; 273:2891–2901. [PubMed: 16817851]

Slominski A, Semak I, Zjawiony J, Wortsman J, Gandy MN, Li J, Zbytek B, Li W, Tuckey RC. Enzymatic metabolism of ergosterol by cytochrome p450scc to biologically active 17alpha,24-dihydroxyergosterol. Chem Biol. 2005a; 12:931–939. [PubMed: 16125105]

Slominski A, Semak I, Zjawiony J, Wortsman J, Li W, Szczesniewski A, Tuckey RC. The cytochrome P450scc system opens an alternate pathway of vitamin D3 metabolism. FEBS J. 2005b; 272:4080–4090. [PubMed: 16098191]

Slominski A, Wortsman J, Paus R, Elias PM, Tobin DJ, Feingold KR. Skin as an endocrine organ: implications for its function. Drug Discov Today Dis Mech. 2008; 5:137–144. [PubMed: 19492070]

Slominski A, Zjawiony J, Wortsman J, Semak I, Stewart J, Pisarchik A, Sweatman T, Marcos J, Dunbar CC, Tuckey R. A novel pathway for sequential transformation of 7-dehydrocholesterol and expression of the P450scc system in mammalian skin. Eur J Biochem. 2004; 271:4178–4188. [PubMed: 15511223]

Slominski AT, Janjetovic Z, Fuller BE, Zmijewski MA, Tuckey RC, Nguyen MN, Sweatman T, Li W, Zjawiony J, Miller D, Chen TC, Lozanski G, Holick MF. Products of vitamin D3 or 7-

dehydrocholesterol metabolism by cytochrome P450scc show anti-leukemia effects, having low or absent calcemic activity. PLoS One. 2010; 5:e9907. [PubMed: 20360850]

Slominski AT, Kim T-K, Shehabi HZ, Semak I, Tang EKY, Nguyen MN, Benson HAE, Korik E, Janjetovic Z, Chen J, Yates CR, Postlethwaite A, Li W, Tuckey RC. In vivo evidence for a novel pathway of vitamin D3 metabolism initiated by P450scc and modified by CYP27B1. FASEB J. 2012a

Slominski AT, Kim TK, Janjetovic Z, Tuckey RC, Bieniek R, Yue J, Li W, Chen J, Nguyen MN, Tang EK, Miller D, Chen TC, Holick M. 20-Hydroxyvitamin D2 is a noncalcemic analog of vitamin D with potent antiproliferative and prodifferentiation activities in normal and malignant cells. Am J Physiol Cell Physiol. 2011a; 300:C526–C541. [PubMed: 21160030]

Slominski AT, Li W, Bhattacharya SK, Smith RA, Johnson PL, Chen J, Nelson KE, Tuckey RC, Miller D, Jiao Y, Gu W, Postlethwaite AE. Vitamin D analogs 17,20S(OH)2pD and 17,20ROH)2pD are noncalcemic and exhibit antifibrotic activity. J Invest Dermatol. 2011b; 131:1167–1169. [PubMed: 21228816]

Slominski AT, Zmijewski MA, Semak I, Sweatman T, Janjetovic Z, Li W, Zjawiony JK, Tuckey RC. Sequential metabolism of 7-dehydrocholesterol to steroidal 5,7-dienes in adrenal glands and its biological implication in the skin. PLoS One. 2009; 4:e4309. [PubMed: 19190754]

Slominski AT, Zmijewski MA, Skobowiat C, Zbytek B, Slominski RM, Steketee JD. Sensing the Environment: Regulation of Local and Global Homeostasis by the Skin's Neuroendocrine System. Advances in Anatomy, Embryology and Cell Biology. 2012b; 212:1–115.

Smith DW, Lemli L, Opitz JM. A Newly Recognized Syndrome of Multiple Congenital Anomalies. J Pediatr. 1964; 64:210–217. [PubMed: 14119520]

Strushkevich N, MacKenzie F, Cherkesova T, Grabovec I, Usanov S, Park HW. Structural basis for pregnenolone biosynthesis by the mitochondrial monooxygenase system. Proc Natl Acad Sci U S A. 2011; 108:10139–10143. [PubMed: 21636783]

Tait AD, Hodge LC, Allen WR. Biosynthesis of 3 beta-hydroxy-5,7-pregnadien-20-one by the horse fetal gonad. FEBS Lett. 1983; 153:161–164. [PubMed: 6219005]

Tint GS, Irons M, Elias ER, Batta AK, Frieden R, Chen TS, Salen G. Defective cholesterol biosynthesis associated with the Smith-Lemli-Opitz syndrome. N Engl J Med. 1994; 330:107–113. [PubMed: 8259166]

Tuckey RC. Progesterone synthesis by the human placenta. Placenta. 2005; 26:273–281. [PubMed: 15823613]

Tuckey RC, Bose HS, Czerwionka I, Miller WL. Molten globule structure and steroidogenic activity of N-218 MLN64 in human placental mitochondria. Endocrinology. 2004; 145:1700–1707. [PubMed: 14715710]

Tuckey RC, Cameron KJ. Catalytic properties of cytochrome P-450scc purified from the human placenta: comparison to bovine cytochrome P-450scc. Biochim Biophys Acta. 1993a; 1163:185–194. [PubMed: 8490050]

Tuckey RC, Cameron KJ. Human placental cholesterol side-chain cleavage: enzymatic synthesis of (22R)-20 alpha,22-dihydroxycholesterol. Steroids. 1993b; 58:230–233. [PubMed: 8356576]

Tuckey RC, Li W, Zjawiony JK, Zmijewski MA, Nguyen MN, Sweatman T, Miller D, Slominski A. Pathways and products for the metabolism of vitamin D3 by cytochrome P450scc. FEBS J. 2008a; 275:2585–2596. [PubMed: 18410379]

Tuckey RC, Nguyen MN, Slominski A. Kinetics of vitamin D3 metabolism by cytochrome P450scc (CYP11A1) in phospholipid vesicles and cyclodextrin. Int J Biochem Cell Biol. 2008b; 40:2619–2626. [PubMed: 18573681]

Tuckey RC, Woods ST, Tajbakhsh M. Electron transfer to cytochrome P-450scc limits cholesterol-side-chain-cleavage activity in the human placenta. Eur J Biochem. 1997; 244:835–839. [PubMed: 9108254]

Woods ST, Sadleir J, Downs T, Triantopoulos T, Headlam MJ, Tuckey RC. Expression of catalytically active human cytochrome p450scc in Escherichia coli and mutagenesis of isoleucine-462. Archives of biochemistry and biophysics. 1998; 353:109–115. [PubMed: 9578606]

Zbytek B, Janjetovic Z, Tuckey RC, Zmijewski MA, Sweatman TW, Jones E, Nguyen MN, Slominski AT. 20-Hydroxyvitamin D3, a product of vitamin D3 hydroxylation by cytochrome P450scc,

stimulates keratinocyte differentiation. J Invest Dermatol. 2008; 128:2271–2280. [PubMed: 18368131]

Zmijewski MA, Li W, Chen J, Kim TK, Zjawiony JK, Sweatman TW, Miller DD, Slominski AT. Synthesis and photochemical transformation of 3beta, 21-dihydroxypregna-5,7-dien-20-one to novel secosteroids that show anti-melanoma activity. Steroids. 2011; 76:193–203. [PubMed: 21070794]

Zmijewski MA, Li W, Zjawiony JK, Sweatman TW, Chen J, Miller DD, Slominski AT. Synthesis and photo-conversion of androsta- and pregna-5,7-dienes to vitamin D3-like derivatives. Photochem Photobiol Sci. 2008; 7:1570–1576. [PubMed: 19037511]

Zmijewski MA, Li W, Zjawiony JK, Sweatman TW, Chen J, Miller DD, Slominski AT. Photo-conversion of two epimers (20R and 20S) of pregna-5,7-diene-3beta, 17alpha, 20-triol and their bioactivity in melanoma cells. Steroids. 2009; 74:218–228. [PubMed: 19028513]

Highlights

- Human placenta metabolizes exogenous 7DHC to 7DHP

- Epidermal keratinocytes metabolize both exogenous and endogenous 7DHC to 7DHP

- Intermediates of the pathway are 22(OH)7DHC and 20,22(OH)$_2$7DHC

- 7DHP is metabolized to 7-dehydroprogesterone and hydroxy7DHP

- 7DHP inhibits keratinocyte proliferation
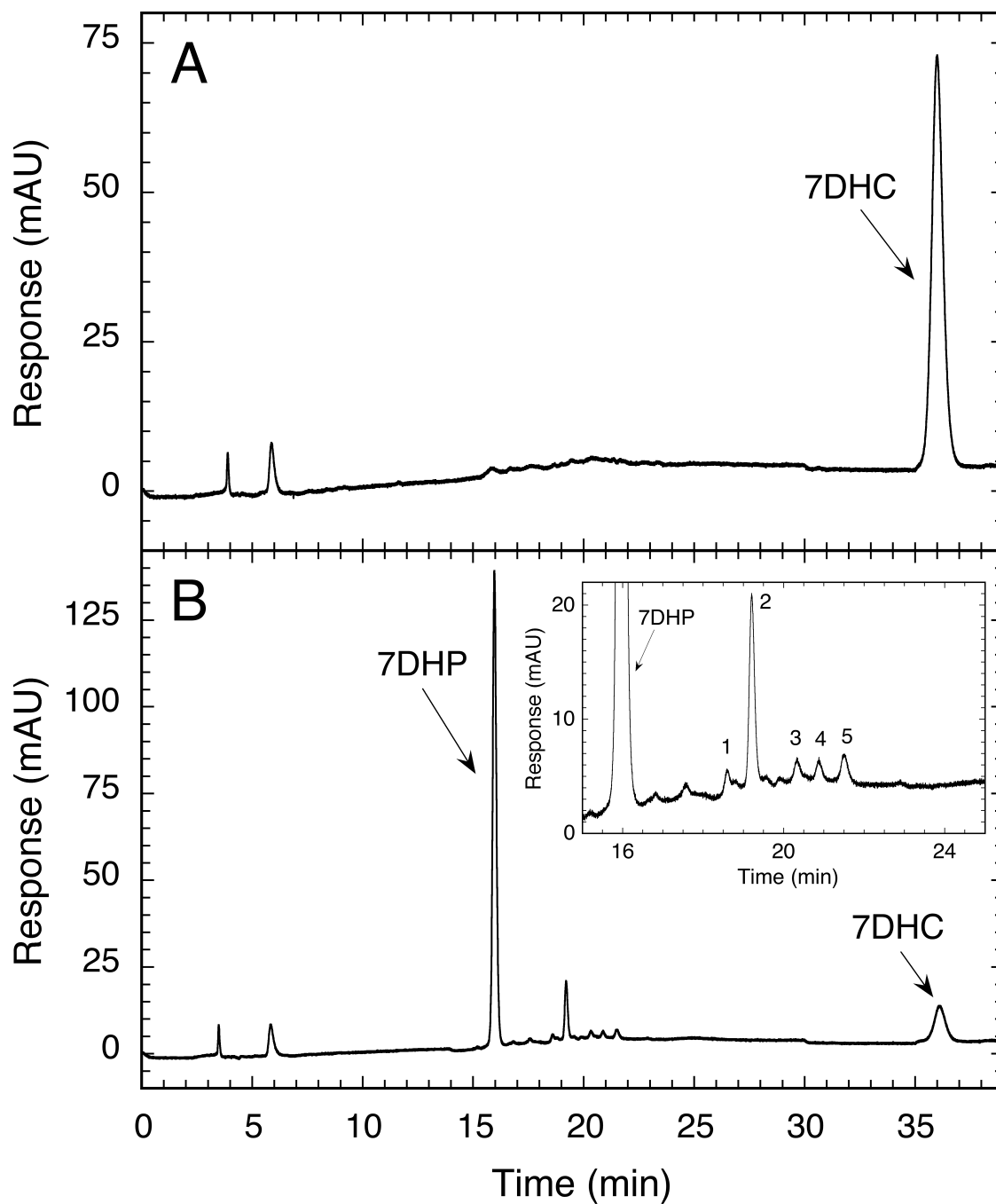
Figure 1.
Production of reaction intermediates by purified human P450scc incubated with 7DHC.
Human cytochrome P450scc was incubated with 200 μM 7DHC in buffer containing 0.9%
2-hydroxypropyl-β-cyclodextrin, 0.4 μM adrenodoxin reductase and 50 μM NADPH in the
absence (control, A) or presence (test, B) of 15 μM adrenodoxin, for 5 min at 37°C. Products
were separated by HPLC as described in the Materials and Methods. The inset in B is an
expansion of the region of the chromatogram showing products additional to 7DHP.
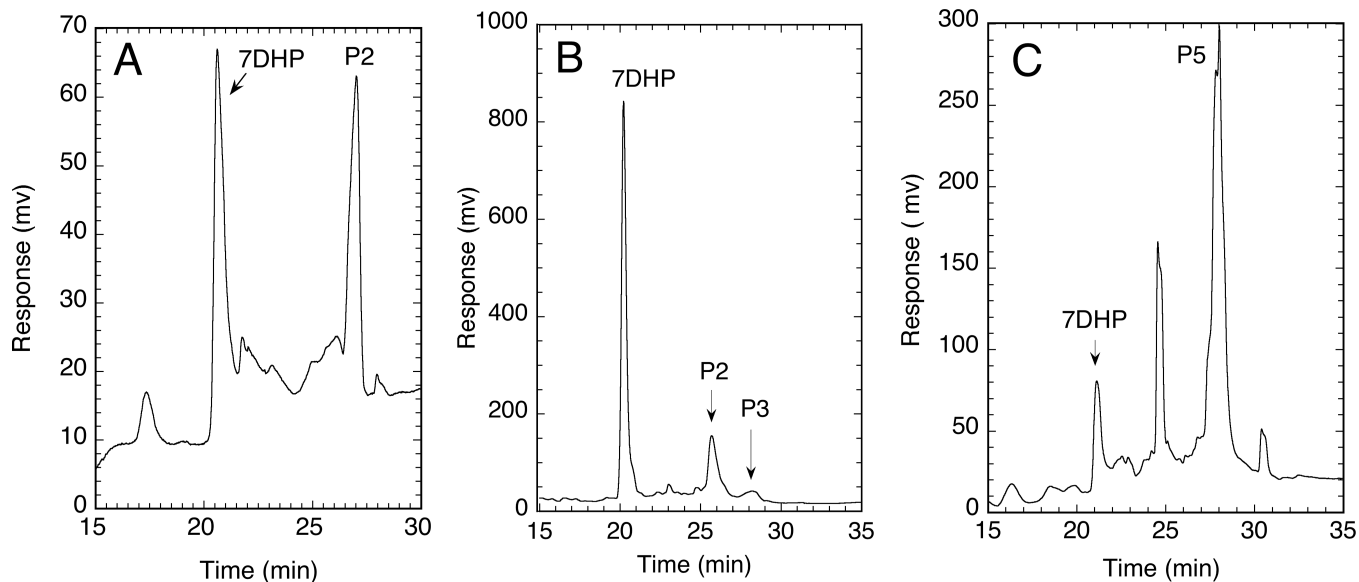
Figure 2.
Metabolism of hydroxy-7DHC products of P450 action on 7DHC, by purified human P450scc. Human P450scc was incubated for 20 min with vesicles containing hydroxy-7DHC products at a ratio of 0.025 mol sterol/mol phospholipid. Substrates and products were separated by HPLC as described in the Materials and Methods. The hydroxy-7DHC derivatives tested for further metabolism by P450scc are labelled according to Fig. 1: A, product 2 (P2); B, product 3 (P3); C, product 5 (P5). No metabolites were seen in control incubations where adrenodoxin was omitted, not shown but similar to Fig. 1A.
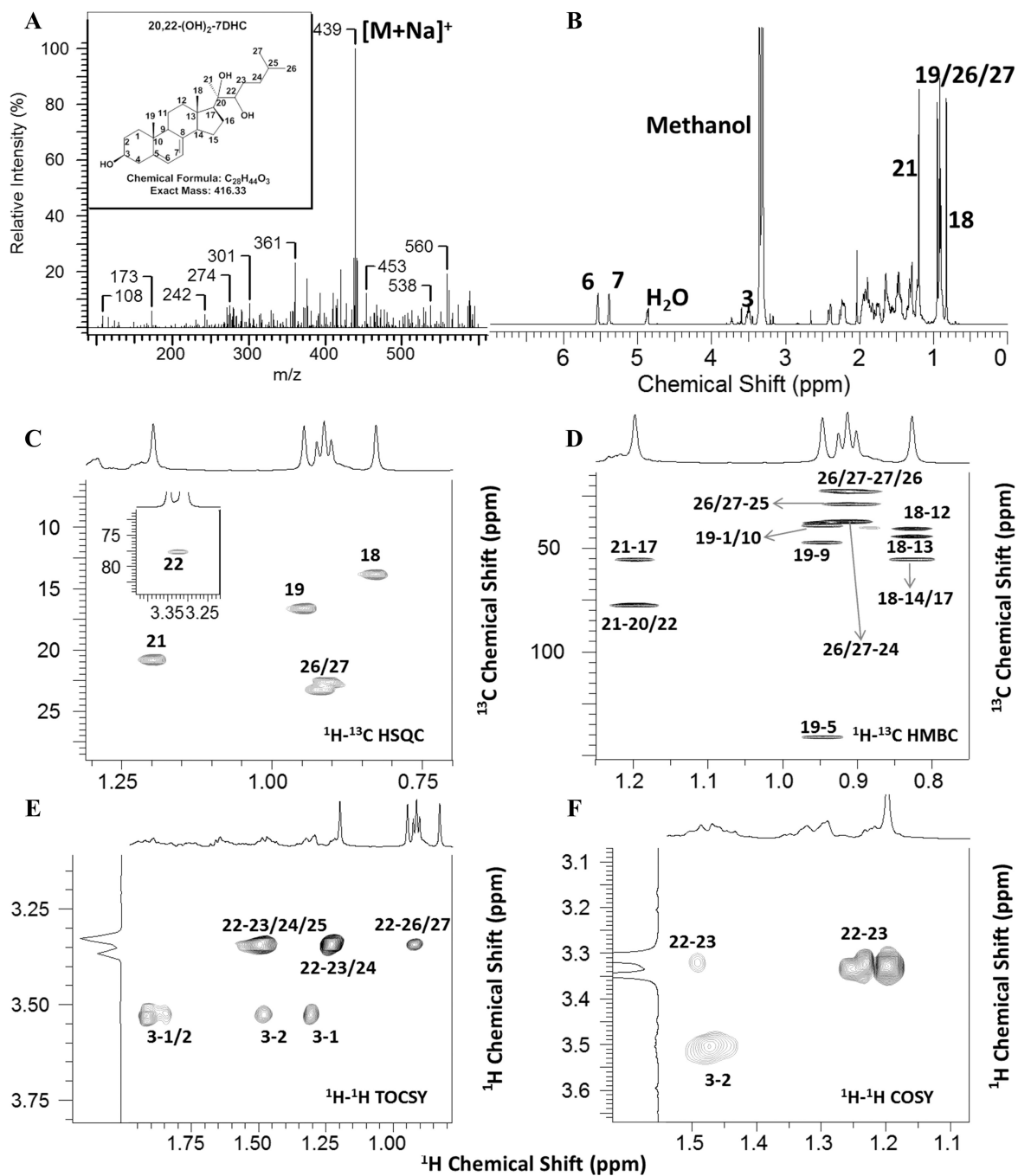
Figure 3.
MASS and NMR spectra of 20,22(OH)$_2$7DHC. (A) MASS; (B)1D Proton; (C) ^{1}H-^{13}C HSQC; (D) ^{1}H-^{13}C HMBC; (E) ^{1}H-^{1}H TOCSY; (F) ^{1}H-^{1}H COSY. Full spectra are shown in Supplemental Figures (Fig. S1-6).
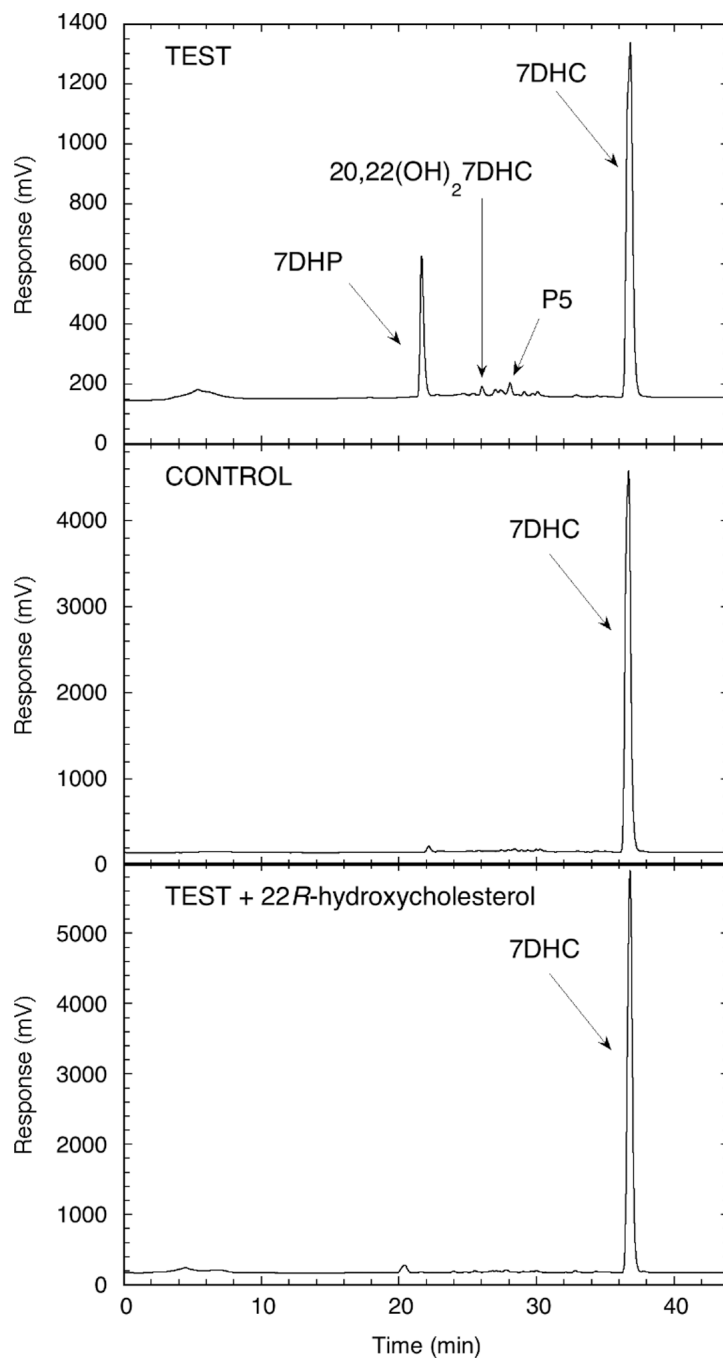
Figure 4.
HPLC chromatograms showing metabolism of 7DHC to 7DHP by placental mitochondria. TEST, mitochondria were incubated with 200 μM 7DHC and 5 μM N-62 StAR protein for 2 h at 37°C. CONTROL, the reaction was stopped at zero time, prior to starting the reaction with isocitrate. TEST + 22R-hydroxycholesterol, 100 μM 22R-hydroxycholesterol was included in the Test incubation.
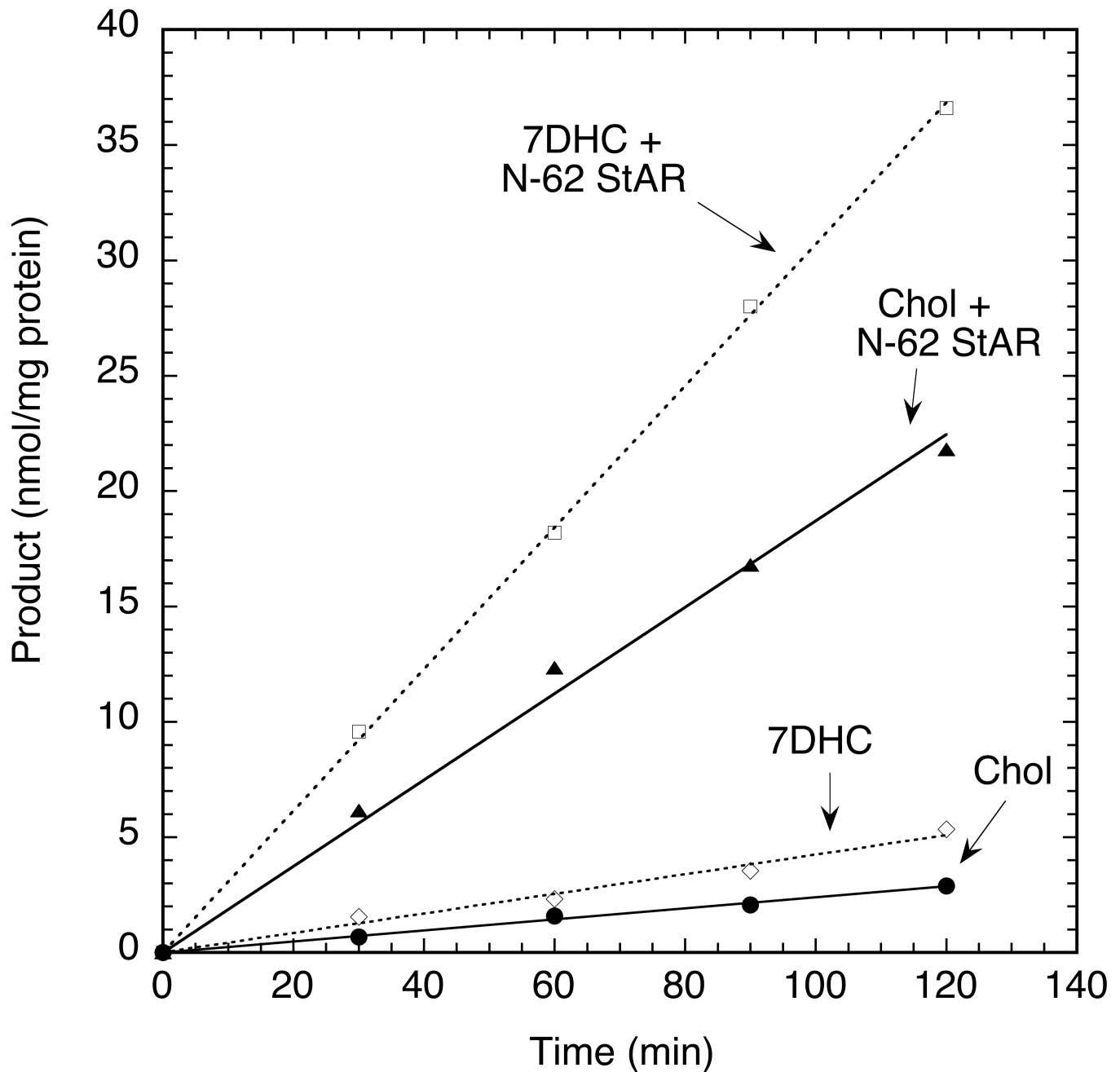
Figure 5.
Time courses for metabolism of exogenous 7DHP and cholesterol by placental mitochondria. Mitochondria were incubated with either 200 μM 7DHC or 200 μM [4-^{14}C]cholesterol (Chol) in the presence or absence of N-62 StAR protein. 7DHP production from 7DHC was measured by HPLC at 280 nm and [4-^{14}C]pregnenolone production from [4-^{14}C]cholesterol was measured by scintillation counting following TLC separation.
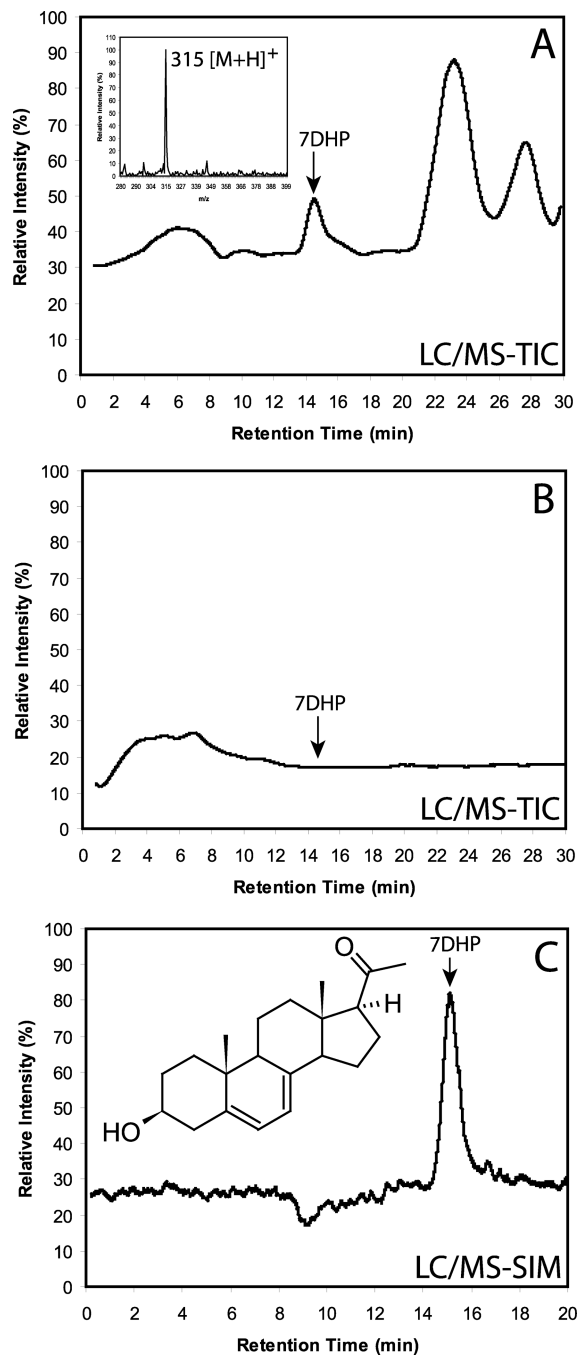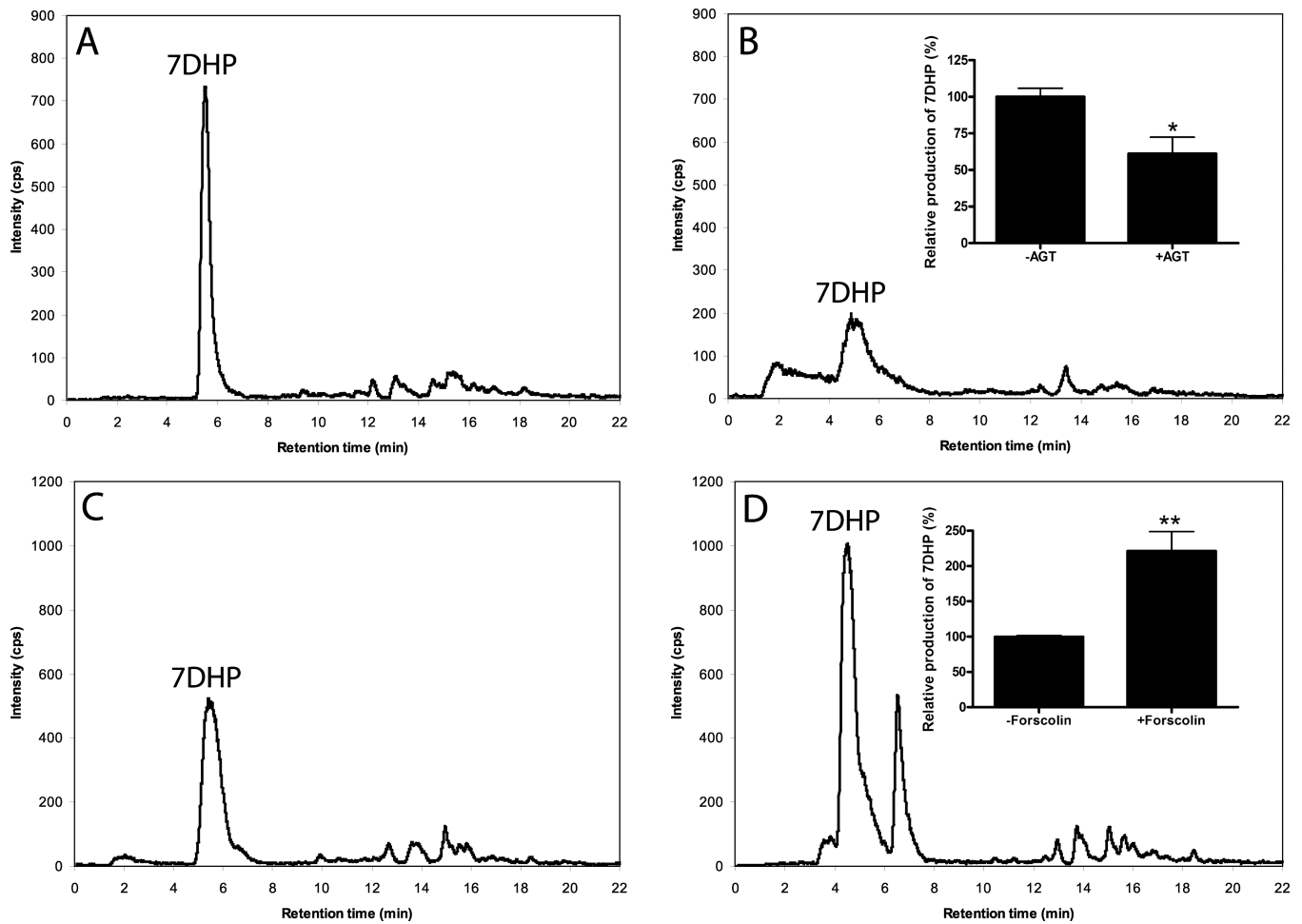
Figure 6.
Detection of 7DHP in human placenta fragments incubated with 7DHC for 20 h. The production of 7DHP was determined by both LC/MS-TIC (A) and LC/MS-SIM (C) and was absent in the control incubation without substrate (B). The arrow shows the retention time corresponding to 7DHP standard.
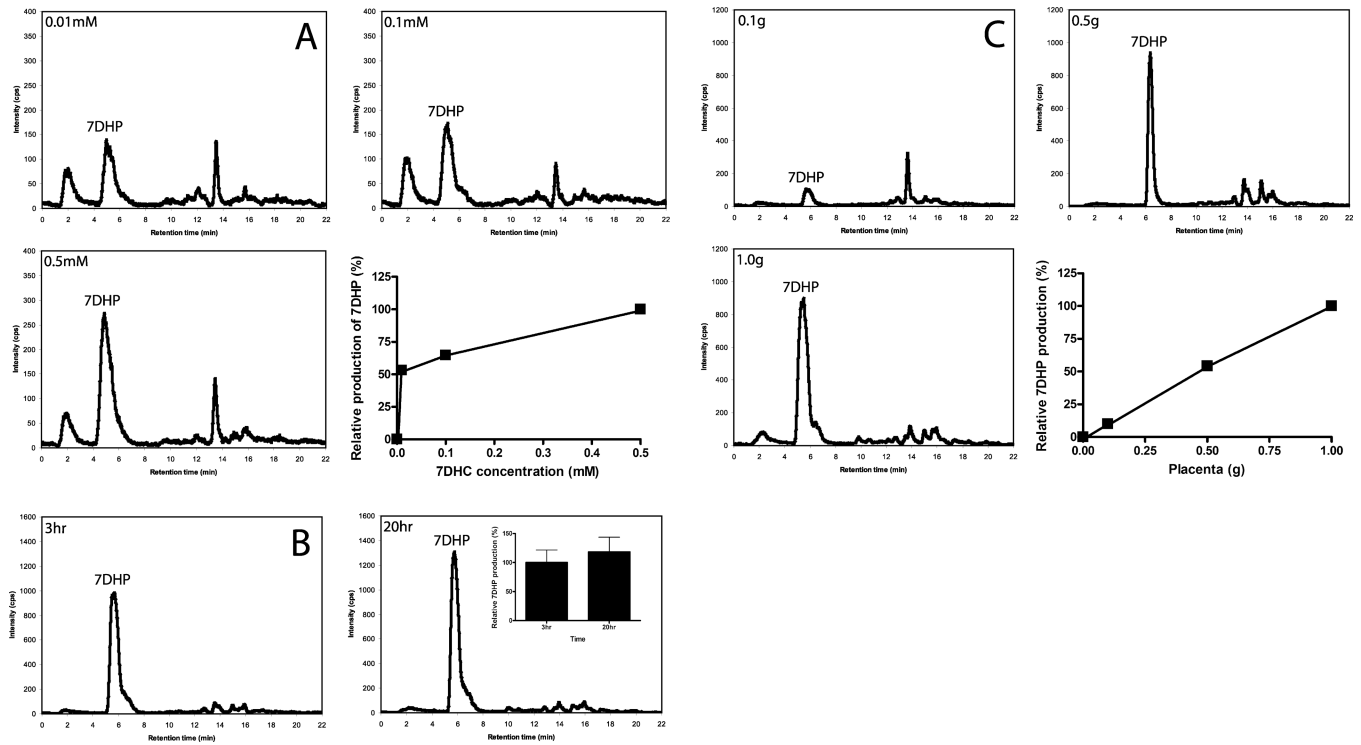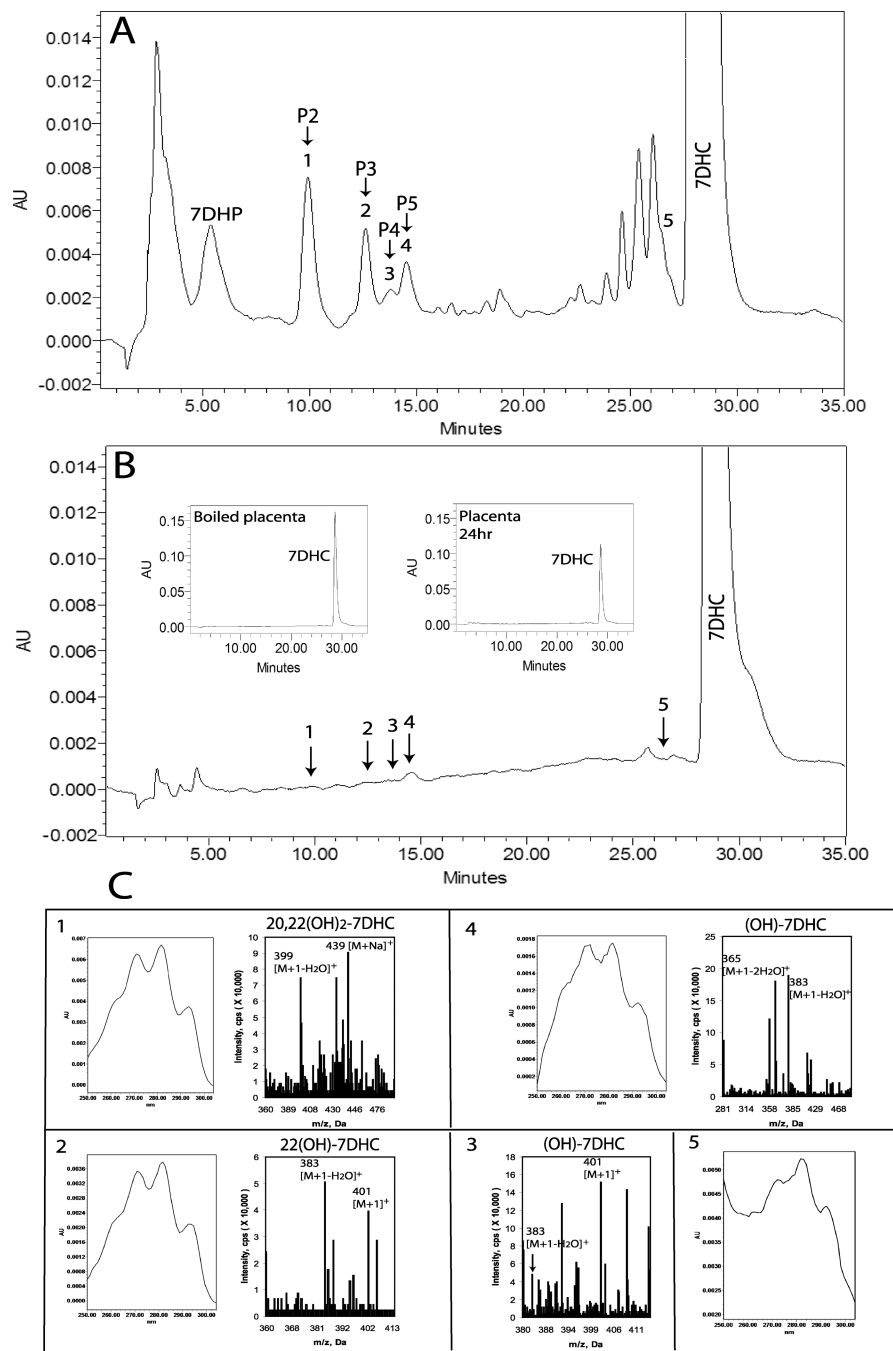
Figure 7.
Transformation of 7DHC to 7DHP in placentas is dependent on substrate concentration (A), incubation time (B), the amount of tissues in the incubation mixture (C). Production of 7DHP by placental fragments was monitored by LC/MS-SIM. Lower right panels in A and C and inset in B show mean values in relation to 7DHC concentration, incubation time and amount of tissue, respectively. The incubation time for the amount of tissue (A) and substrate concentration (C) are 20 h.
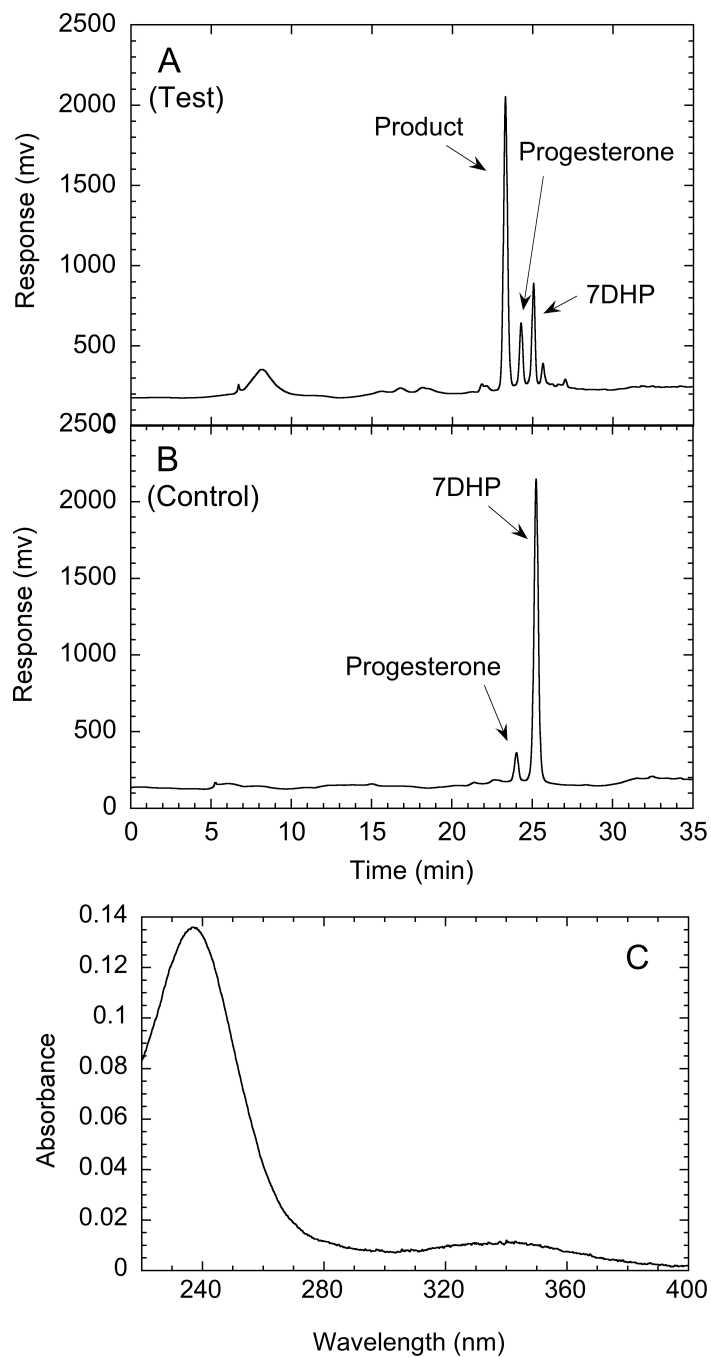
Figure 8.
Production of 7DHP is inhibited by 200 μM DL-aminoglutethimide (AGT) (A, B) and stimulated by 100 μM forskolin (C,D). LC/MS-SIM analysis shows relative concentrations of 7DHP in placentas incubated with 7DHC only (A and C) or 7DHC plus AGT (B) or plus forskolin (D). The inset shows means value −/+SEM (n=3). The incubation time is 20 h.
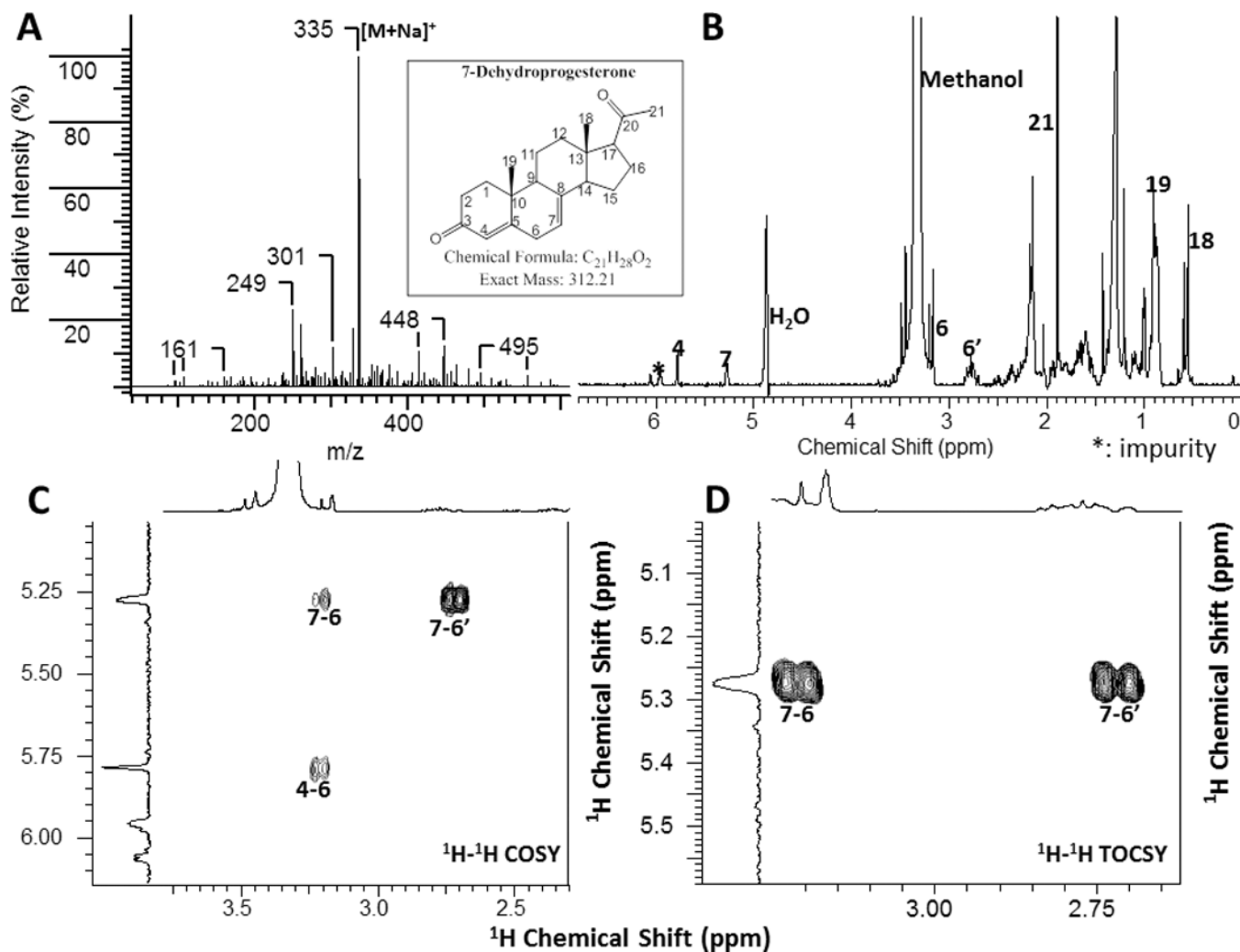
Figure 9.
Identification of 5,7-dienal intermediates of 7DHC metabolism to 7DHP. A, Placenta incubated with 1 mM 7DHC for 24 h. B. Boiled placenta incubated with 1 mM 7DHC for 24 h with an inset showing total consumption of 7DHC. C. UV and mass spectra of the four metabolites detected.
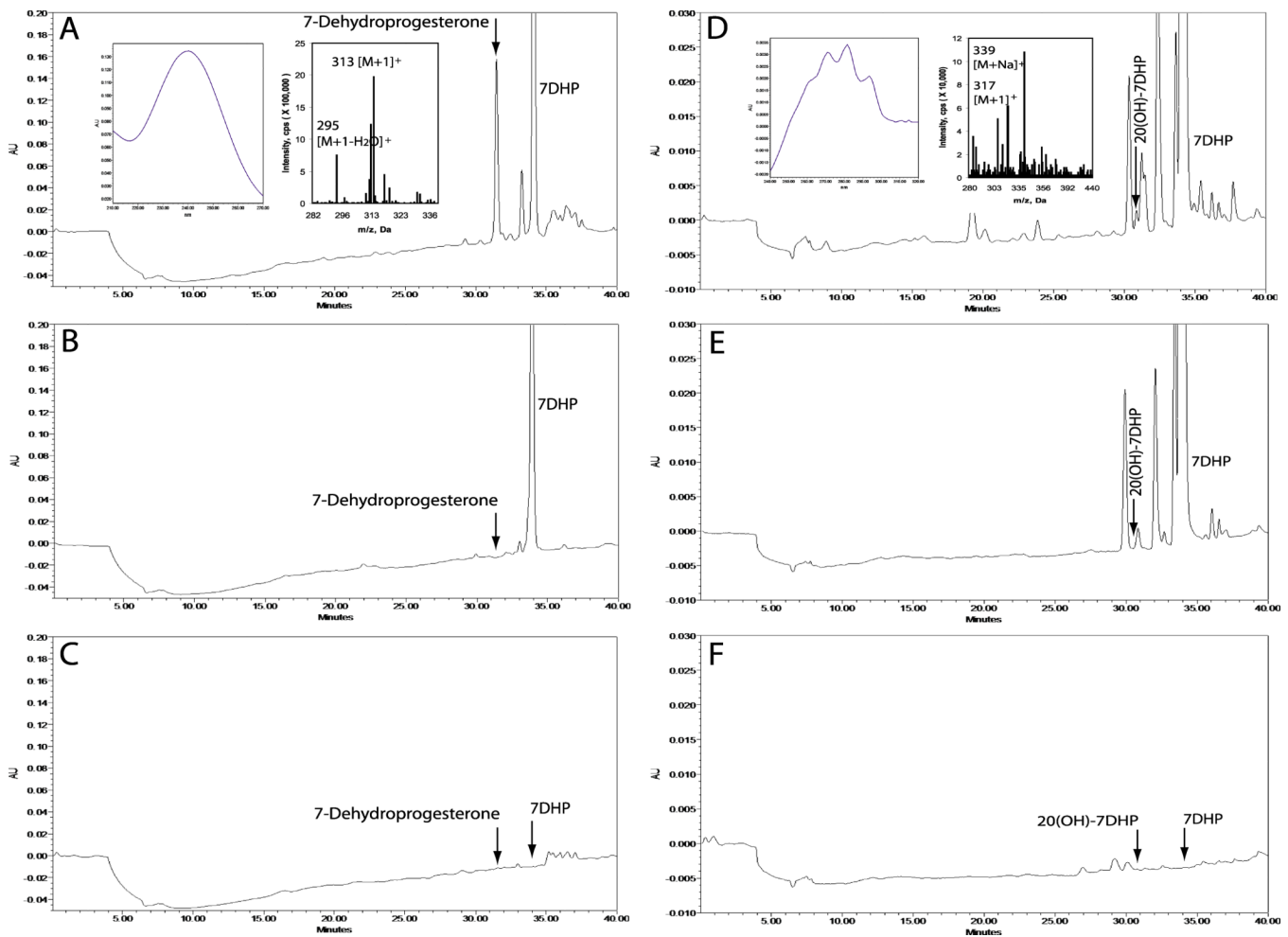
Figure 10.
Placental microsomes metabolize 7DHP. Placental microsomes were incubated with 100 μM 7DHP in the presence of NAD$^+$ for 10 min and products analyzed by reverse phase HPLC. A, Test reaction; B, control reaction carried out as for the test except that 16 μM cyanoketone was present; C, spectrum of the major product recorded after HPLC purification, removal of HPLC solvent (a few h at room temperature under a gentle stream of nitrogen) and dissolving in ethanol.
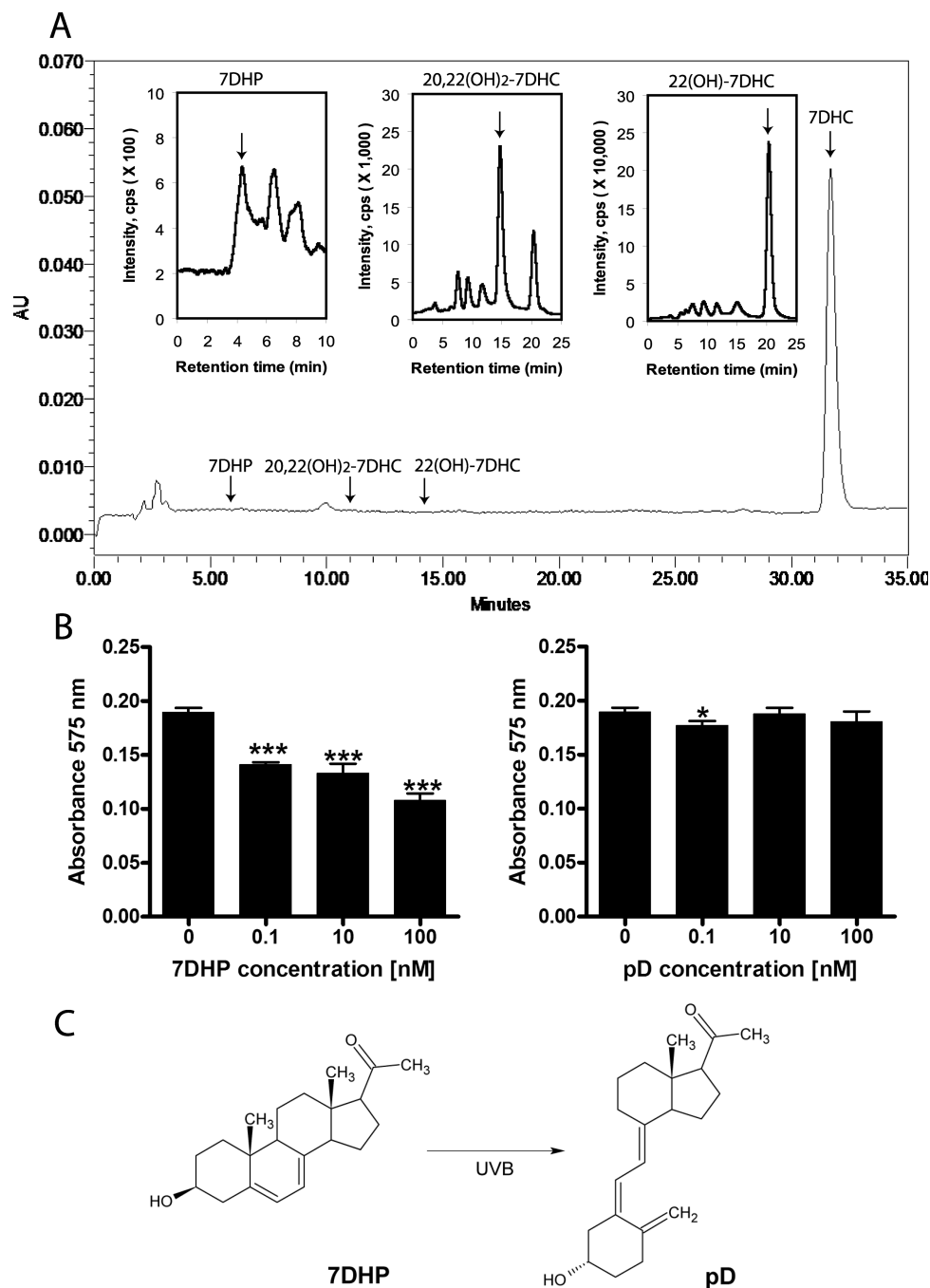
Figure 11.
MASS (A) and NMR (B-D) spectra of 7-dehydroprogesterone produce d by placental microsomes. A, MS identify the molecular ion of 335 [M + Na]+ consistent with real mass (MW=312) of 7-dehydroprogesterone. B, 1H NMR; C, 1H-1H COSY and D, 1H-1H TOCSY spectra.

Figure 12.
Ex-utero transformation of 7DHP to 7-dehydroprogestrone (A) and to monohydroxy-7DHP tentatively assigned as 20(OH)7DHP (D) by placental fragments. A and D, Placenta incubated with 1 mM 7DHP for 20 h. B and E, Boiled placenta incubated with 1 mM 7DHP for 20 h. C and F, Placenta incubated without substrate for 20 h. The chromatogram was monitored at 240nm for 7-dehydroprogesterone (A-C) and 280nm for 20(OH)7DHP (D-F). RP-HPLC was performed using Waters C18 column (250×4.6 mm, 5μm particle size). Elution was carried out with a gradient of methanol in water (50%–100%) at a flow rate 0.35 ml/min (30 min), followed by a wash with 100% methanol (10 min). Other conditions are described in materials and methods.
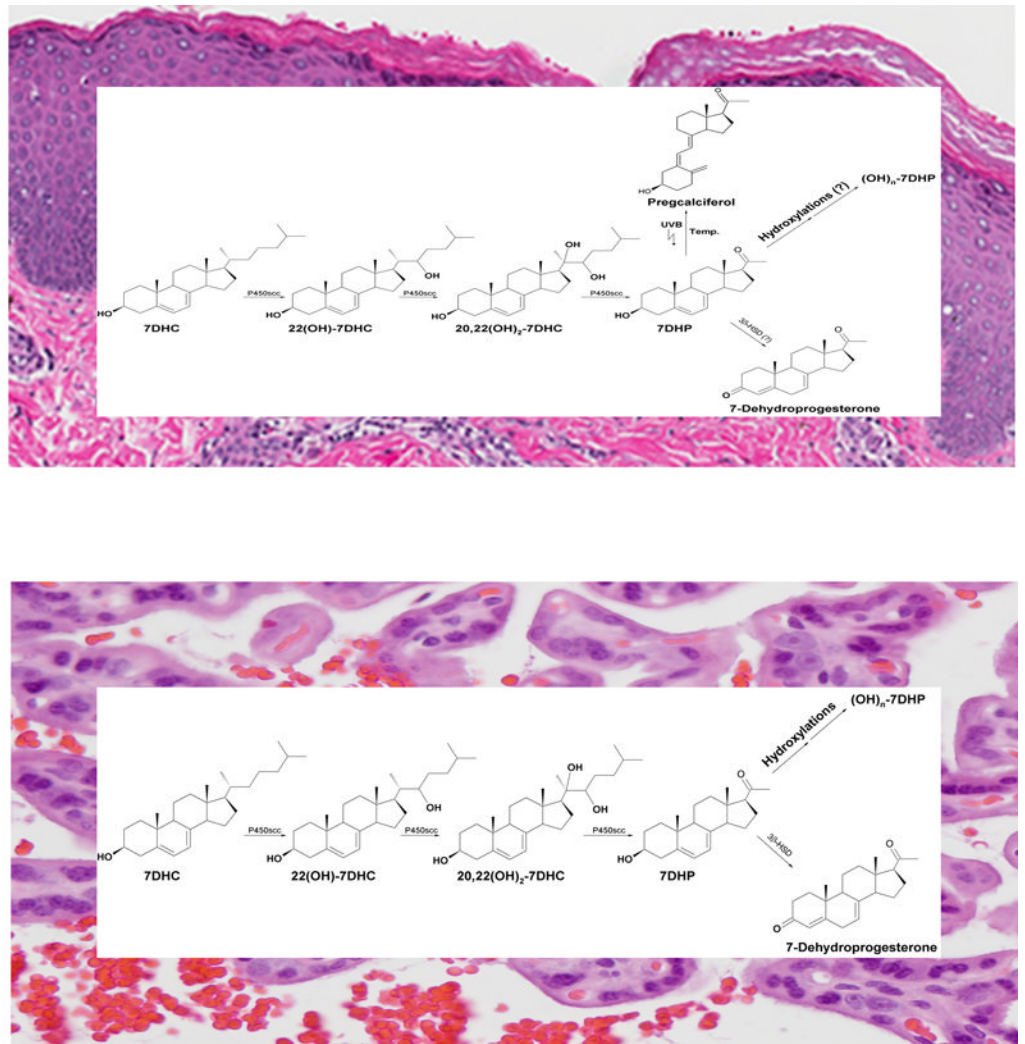
Figure 13.
Endogenous metabolism of 7DHC to 7DHP in epidermal keratinocytes and biological activity of 7DHP.

A. Endogenous production of 22(OH)7DHC, 20,22(OH)$_2$7DHC and 7DHP in pig skin cells. Epidermal keratinocytes isolated from pig skin were incubated ex- vivo for 20 h, extracted with methylene chloride and extracts analyzed by HPLC and LCMS as described before (Slominski et al., 2012a). Inserts show analysis by LCMS with APCI in the MRM mode for 7DHP (MRM: m/z = 315 → 297), and in the SIM mode for 20,22(OH)$_2$7DHC (SIM: m/z = 417) and 22(OH)7DHC (SIM: m/z = 401).

B. 7DHP show antiproliferative activity against HaCaT keratinocytes, while the product of its phototransformation, pregnacalciferol (pD), has little activity.

C. Scheme showing UVB induced conversion of 7DHP to pD.

Figure 14.
Proposed pathways of 7DHC and 7DHP metabolism in placenta (lower panel) and skin (upper panel).

Table 1

NMR chemical shift assignments for 20,22(OH)$_2$7DHC by analysis of their 2D NMR spectra. (Solvent: CD$_3$OD)

20,22(OH)$_2$-7DHC

Atom #	1	2	3	4	5	6
^{1}H	1.30α, 1.91β	1.84α, 1.47β	3.51	2.41α, 2.25β	NA	5.54
^{13}C	39.6	32.6	70.9	41.4	140.5	120.5

Atom #	7	8	9	10	11	12
^{1}H	5.38	NA	1.97	NA	1.63α, 1.78β	1.35α, 2.22β
^{13}C	117.8	141.2	47.4	38	22	40.8

Atom #	13	14	15	16	17	18
^{1}H	NA	1.9	1.75α, 1.46β	1.63α, 1.94β	1.65	0.83
^{13}C	44.6	55.7	23.8	21.9	55.9	13.8

Atom #	19	20	21	22	23	24
^{1}H	0.95	NA	1.2	3.32	1.50, 1.22	1.47, 1.22
^{13}C	16.6	77.7	20.8	77.6	30.4	37.5

Atom #	25	26	27
^{1}H	1.57	0.92	0.91
^{13}C	29.1	22.7	22.7

NA – Not applicable (ternary carbons).